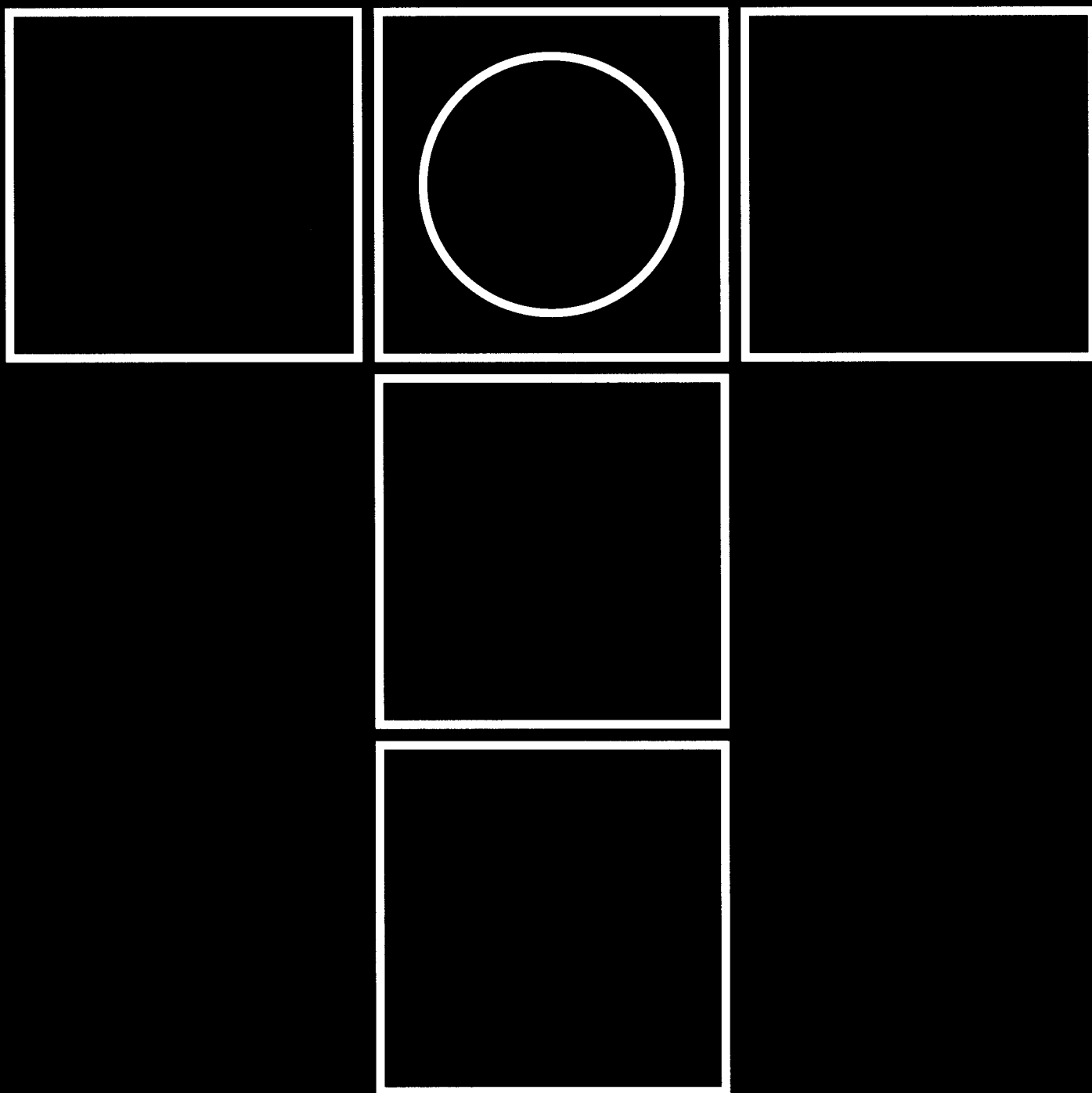


tribology in industry

YU ISSN 0354 - 8996
VOLUME 21
MARCH 1999.

1



tribology in industry



contents



INTRODUCTION	B. IVKOVIĆ: tribology in industry at the 21st century threshold . . .	3
RESEARCH	M. R. JANKOVIĆ: Non-dimensional Design Parameter of Porous Metal Slide Bearings	5
	B. TADIĆ, S. MITROVIĆ: Thin-walled Pipes Bending by Application of Friction Generated Heat	8
	I. KLIANAR, A. STEFANOVIĆ, M. RAJKOVIĆ: Possibilities of Piston-cylinder Diagnostics of Fits of Motors	12
	N. BURNETE, A. CAZILA, N. BATAGA, V.T. POP: Research Regarding The Piston Longitudinal Profile Influence on The Displacement of The Cylinder Relative to The Cylinder Block	17
	I. MUSCA: Lubricant Compressibility - Theoretical and Experimental Aspects	21
	L. V. SEVERIN, M. A. TEODORESCU, D. AMARANDEI: Friction Influence on The Uniformity Deformation Coefficient in The Cold Forming Ball Bearing Semi-cages	25
	J. VLADIĆ: Influence of Tribological Processes on The Safety Concerning The Slipping of Steel Rope over The Driving Pulley . . .	30
NEWS	35
BOOKS AND JOURNALS	36
SCIENTIFIC MEETINGS	37

Tribology in Industry at the 21st century threshold

In the past twenty years journal *Tribology in Industry* has regularly been published quarterly, as the first and still the only journal of this kind on the territory of former Yugoslavia, regardless of all the changes that occurred here in the meantime, both in political and economic sense. The last two issues published in 1998. (September and December issue), have presented, among others, the structure and number of scientific papers in which were, in the past period, published results of tribological research, realized on Yugoslav territory and also in other industrial countries.

In this year 1999, the journal *Tribology in Industry* begins its third decade, unfortunately in the most difficult conditions so far. The state of war in our country that is in force since March prevented publishing of this year's first issue, though it was already prepared for printing. This is the main reason that the March issue of our journal appears in June.

Besides the issue in Serbian, with abstracts in English and Russian, the Editorial Board, with approval and on initiative of the Yugoslav Tribology Society Executive Board, prepares and publishes, since 1997, also the issue in English entitled *Tribology in Industry* with the separate ISSN number. The Editor of this issue also is Faculty of Mechanical Engineering in Kragujevac.

In its third decade, which mainly coincides, with the first decade of the 21st century, the journal's Editorial Board obligation is, to the great extent, to enrich contents of its both issues. This does not only apply to the most important part of the journal in which are being published scientific research results, realized in the area of tribology, but also to those portions of the journal in which are presented, to the scientific and expert public, news from the world of tribology, both of the expert and informative characters.

Into the new century, tribology as a science and technology about the processes of friction, wear and lubrication of the tribo-mechanical systems enters with numerous research programs that are to the great extent related to micro and nano-tribology. Contemporary measuring equipment, like the AFM/FFM (Atomic Force Microscopy), enables studying of contact surfaces at the levels of atomic and molecular sizes, namely the nanometers level. Studies of contact surfaces roughness, phenomena of adhesion, friction, wear, contact layers destruction, limiting lubrication and material transfer in the contact zone between tribo-mechanical systems elements and environment, will be conducted at the nanometers level, with help of this instrumentation and the new measuring systems, whose development is expected in

the forthcoming years. Many contact surfaces of tribo-mechanical systems elements are going to be machined, in the coming century, by the new machining processes, that belong to nano-technology which was developed in the past few years in industrial world.

In expert literature, especially in scientific type journals and proceedings of papers presented at numerous scientific conferences, one can more and more frequently come across the opinion that basic restrictions for further development of industrial productions in the 21st century would lie mainly in tribological characteristics of tribo-mechanical systems elements. Many mechanical systems (production and other equipment, transportation means, etc.) will operate in the future under more severe conditions than today. Outside loads of the contact zone in tribo-mechanical systems are going to be increased, and the relative velocities as well as aggressiveness of environment in which the contact is realized. At the same time, necessity of greater system's productivity, increase of the energy efficiency ratio with simultaneous decrease of energy consumption in tribo-mechanical systems functioning, are constantly going to rise in all the areas of industrial production and transportation. These requirements can be satisfied only by increasing the wear resistance of the

contact layers of the tribo-mechanical systems elements, by improvement of their characteristics from the aspect of fatigue as well as by increase of their load carrying capacity.

In the years to come, besides growing application of tribological coatings of existing types, and other procedures for contact layers characteristics, it is also expected the significant application of the Duplex methods for coatings deposition. Research, conducted until now, have shown that, for instance, wear resistance of contact layers created by the PVD TiN coating and nitriding (Duplex system - coating / nitriding), is far bigger than wear resistance of contact layers created only by PVD TiN coating or application of the nitriding procedure.

The wear resistance of solid elements of the tribo-mechanical systems depends on, as it is well known, tribological properties of lubricants, which is usually present in the contact zones. Development in the area of lubricants is very intensive; thus, it is expected that their tribological properties are going to be significantly improved in the next decade.

Development and research in the area of tribology impose a necessity for constant quality control of the tribo-mechanical systems solid elements and lubricants, both in the phase of their development and production as well as in the exploitation phase. It is known that it is very hard to create the contact layers of the tribo-mechanical systems elements, or to manufacture lubricants, in such a way that they exhibit excellent tribological characteristics in all the possible contact conditions (different

sliding speeds, loads, temperatures, environmental aggressiveness).

Control of tribological characteristics is a very complex problem that has to be solved with application of extremely precise measuring instrumentation, which would be able to produce sufficiently reliable information of this kind. When the tribological properties of solid materials are concerned, as well as those of coatings, lubricants and procedures for contact layers creation, their determination is almost exclusively done by measuring the friction force in the contact zone and magnitude of wear of the tribo-mechanical system critical element. Appearance of coatings on contact surfaces required development of instrumentation for identification of load at which the destruction of coating occurs, namely destruction of its connection with substrate.

Certain and not very large number of institutes and companies in industrial countries have developed and is already producing several types of tribometers, at which is possible to simulate conditions of realization of contact in real tribo-mechanical systems, both in production equipment and transportation means. Tribometers like Pin-on-Disc, Block-on-Disc, Four-Ball, and many others, are aimed for simulation of contacts in specific tribo-mechanical systems, and they find their application in all the major companies and laboratories. Their development, however, is not finished. Almost every year new tribometers appear, with certain improvements that are related to their functioning and automatic processing of experimental results. Special problem, that appears with almost all

tribometers, is related to measurement of critical elements wear magnitude, is today solved by application of laser sounding tubes, or extremely precise measuring systems for measurement of linear displacements.

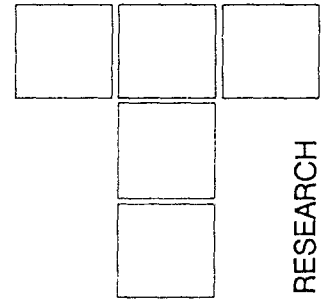
University laboratories in Yugoslavia, as well as laboratories in independent institutes, are very poor with this type of measuring and research equipment. In two companies that are dealing with manufacturing lubricants in our country situation is somewhat better, but it is very far from being able to satisfy needs in this type of operation. Appearance of new small manufacturers of lubricants did not lead to increase of number of tribometers in Yugoslavia.

When tribology in the 21st century is concerned, one fact should not be neglected that knowledge, gathered so far in the area of tribology, is not sufficiently applied in practice. Tribological campaigns are being frequently organized in industrially developed countries, since it was noticed that application of existing tribological knowledge can contribute to better operation of industrial systems, and that without introducing expensive new technologies into the production systems.

Journal Tribology in Industry (Serbian language issue) will continue in trying, within restrictions of its possibilities, to present to domestic scientific and expert public, results of investigations that appear in the area of tribology, not only in our country but also from the world. At the same time journal Tribology in Industry (English language issue) will present results of Yugoslavian tribologists to the world public to a significantly greater extent.

M. R. JANKOVIĆ

Non-dimensional Design Parameter of Porous Metal Slide Bearings



In the papers regarding the hydrodynamics theory of porous metal bearing lubrication, published in well-known journals by the eminent authors such as V. T. Morgan, A. Cameron, A. E. Stainsby, W. T. Rouleau, P. R. K. Murti and C. Cusano, the non-dimensional design parameter (Ψ) is emphasized as one of the most important parameters.

In diagrams showing dependency of the capacity, relative load, load angle and friction parameters, this parameter is being treated as an independent variable (abscissa of the diagram).

Besides geometry, Ψ - parameter also includes the open porosity (P), represented indirectly by permeability (Φ) of porous bearing material. In [1], experimental dependence of permeability (Φ) on its open porosity (Ψ): $\Phi = f(P)$, was shown for bronze with 1.5 % of graphite.

This author has calculated the design non-dimensional parameter and is showing the values obtained in tables and diagrams, for bearings made of bronze with 1.5 %G of graphite, which are made and used in electromotor-industry, all over Yugoslavia.

Keywords: Metal Slide Bearings, Non-dimensional (permeability) parameter

NOMENCLATURE

- a - porosity exponent
- C_Φ - coefficient of permeability
- c - radial clearance
- d - journal diameter
- H - wall thickness of porous bearing
- P - porosity of bearing material
- Φ - permeability of bearing material
- Ψ - design (permeability) parameter

ANALYSIS AND RESULTS

In [1], Fig. 89.2, the experimental curves $\Phi = f(P)$ are presented as exponential functions :

$$\Phi = C_\Phi \cdot P^a \quad (1)$$

Using double logarithmic coordinates ($\log P$, $\log \Phi$) instead of usual semi-logarithmic coordinates (P , $\log \Phi$), the exponential curves are becoming linear ones, valid up to 35% porosity.

The following results are obtained Fig. 89.2, [1] from:

$$P_1 = 20\%, \Phi_1 = 0.6 \cdot 10^{-10} \text{ cm}^2 = 0.6 \cdot 10^{-2} \text{ cm}^2$$

$$P_2 = 30\%, \Phi_2 = 9.0 \cdot 10^{-10} \text{ cm}^2 = 9.0 \cdot 10^{-2} \text{ cm}^2$$

Then, the coefficient of porosity (porosity function exponent) is:

$$a = \frac{\frac{\log \Phi_2}{\Phi_1}}{\frac{\log P_2}{P_1}} = \frac{\frac{\log 0.09}{0.006}}{\frac{\log 30}{20}} \approx 6.7 \quad (2)$$

We can calculate C_Φ , from the following condition:

$$\log \Phi = \log C_\Phi + a \log P \quad (3)$$

or:

$$\log C_\Phi = \log \Phi - a \log P \quad (3')$$

$$\log C_\Phi = \log 0.6 \cdot 10^{-2} - 6.7 \log 20 = -10.9387,$$

and after applying inverse logarithmic operation:

$$C_\Phi = 0.115 \cdot 10^{-10} \mu\text{m}^2$$

In this way we can calculate permeability for each value of open porosity of bearings made of bronze with 1.5% of graphite, with the values of $P = (20 \dots 30)\%$, which are obtained in industry.

For the porous bearing shown in Fig. 1, with ratio: $H/d = 0.1 \dots 0.4$ for values ($d = 10 \text{ mm}$, $H = (1 \dots 4) \text{ mm}$), bearing for electromotor, the radial clearance values are:

$$c = (0.25 \dots 0.75) \cdot d \mu\text{m}; \quad (d \text{ in mm}) \quad (4)$$

Dr M. R. Jankovic, associate professor
Faculty of Mechanical Engineering,
University of Belgrade, Yugoslavia

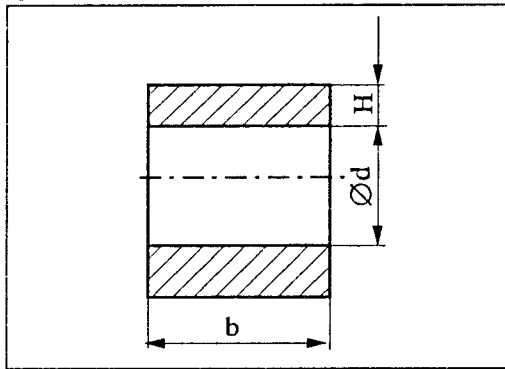


Fig 1. Geometry of porous metal bearing

The calculated values of design non-dimensional parameter (Ψ), according to [1], [2] and [3], are shown in Tables 1 to 4 and in diagram Fig. 2.

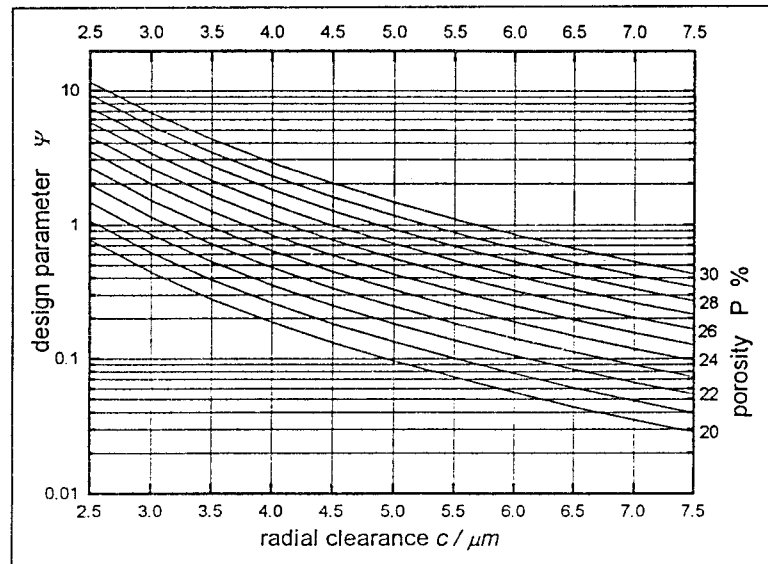


Fig. 2. Design parameter values according to Table 2.

Table 1. Nondimensional Design parameter (Ψ)

P %	20	21	22	23	24	25	26	27	28	29	30
$\Phi 10^2, \mu\text{m}^2$	0.600	0.831	1.135	1.528	2.033	2.672	3.475	4.475	5.710	7.224	9.000
c, μm	$\Psi = \Phi \cdot H / c^3, H = 1 \text{ mm} - \text{wall thickness}$										
2.5	0.383	0.532	0.726	0.978	1.301	1.710	2.224	2.864	3.654	4.623	5.760
3	0.222	0.308	0.420	0.566	0.753	0.990	1.287	1.657	2.115	2.676	3.333
3.5	0.140	0.194	0.265	0.356	0.474	0.623	0.810	1.044	1.332	1.685	2.099
4	0.093	0.130	0.177	0.239	0.318	0.418	0.543	0.699	0.892	1.129	1.406
4.5	0.066	0.091	0.125	0.168	0.223	0.293	0.381	0.491	0.627	0.793	0.988
5	0.048	0.066	0.091	0.122	0.163	0.214	0.278	0.358	0.457	0.578	0.720
5.5	0.036	0.050	0.068	0.092	0.122	0.161	0.209	0.269	0.343	0.434	0.541
6	0.028	0.038	0.053	0.071	0.094	0.124	0.161	0.207	0.264	0.334	0.417
6.5	0.022	0.030	0.041	0.056	0.074	0.097	0.127	0.163	0.208	0.263	0.328
7	0.017	0.024	0.033	0.045	0.059	0.078	0.101	0.130	0.166	0.211	0.262

Table 2. Nondimensional Design parameter (Ψ)

P %	20	21	22	23	24	25	26	27	28	29	30
$\Phi 10^2, \mu\text{m}^2$	0.600	0.831	1.135	1.528	2.033	2.672	3.475	4.475	5.710	7.224	9.000
c, μm	$\Psi = \Phi \cdot H / c^3, H = 2 \text{ mm} - \text{wall thickness}$										
2.5	0.767	1.064	1.453	1.956	2.602	3.420	4.448	5.728	7.309	9.247	11.520
3	0.444	0.616	0.841	1.132	1.506	1.979	2.574	3.315	4.230	5.351	6.667
3.5	0.279	0.388	0.529	0.713	0.948	1.246	1.621	2.087	2.664	3.370	4.198
4	0.187	0.260	0.355	0.477	0.635	0.835	1.086	1.398	1.784	2.257	2.813
4.5	0.131	0.182	0.249	0.335	0.446	0.586	0.763	0.982	1.253	1.586	1.975
5	0.096	0.133	0.182	0.244	0.325	0.428	0.556	0.716	0.914	1.156	1.440
5.5	0.072	0.100	0.136	0.184	0.244	0.321	0.418	0.538	0.686	0.868	1.082
6	0.055	0.077	0.105	0.141	0.188	0.247	0.322	0.414	0.529	0.669	0.833
6.5	0.044	0.061	0.083	0.111	0.148	0.195	0.253	0.326	0.416	0.526	0.655
7	0.035	0.048	0.066	0.089	0.119	0.156	0.203	0.261	0.333	0.421	0.525
7.5	0.028	0.039	0.054	0.072	0.096	0.127	0.165	0.212	0.271	0.342	0.427

Table 3. Nondimensional Design parameter (Ψ)

P %	20	21	22	23	24	25	26	27	28	29	30
$\Phi 10^2, \mu\text{m}^2$	0.600	0.831	1.135	1.528	2.033	2.672	3.475	4.475	5.710	7.224	9.000
c, μm	$\Psi = \Phi \cdot H / c^3, \quad H = 3 \text{ mm} - \text{wall thickness}$										
2.5	1.150	1.596	2.19	2.934	3.903	5.130	6.672	8.592	10.963	13.870	17.280
3	0.666	0.923	1.261	1.698	2.259	2.969	3.861	4.972	6.344	8.072	10.000
3.5	0.419	0.581	0.794	1.069	1.423	1.870	2.431	3.131	3.995	5.055	6.297
4	0.281	0.390	0.532	0.716	0.953	1.252	1.629	2.089	2.677	3.386	4.219
4.5	0.197	0.274	0.374	0.503	0.669	0.880	1.144	1.473	1.880	2.378	2.963
5	0.144	0.199	0.272	0.367	0.488	0.641	0.834	1.074	1.370	1.734	2.160
5.5	0.108	0.150	0.205	0.276	0.367	0.482	0.627	0.807	1.030	1.303	1.623
6	0.083	0.115	0.158	0.212	0.282	0.371	0.483	0.622	0.793	1.003	1.250
6.5	0.065	0.091	0.124	0.167	0.222	0.292	0.380	0.489	0.624	0.789	0.983
7	0.052	0.073	0.099	0.134	0.178	0.234	0.304	0.391	0.499	0.632	0.787
7.5	0.043	0.059	0.081	0.109	0.145	0.190	0.247	0.318	0.406	0.514	0.640

Table 4. Nondimensional Design parameter (Ψ)

P %	20	21	22	23	24	25	26	27	28	29	30
$\Phi 10^2, \mu\text{m}^2$	0.600	0.831	1.135	1.528	2.033	2.672	3.475	4.475	5.710	7.224	9.000
c, μm	$\Psi = \Phi \cdot H / c^3, \quad H = 4 \text{ mm} - \text{wall thickness}$										
2.5	1.533	2.127	2.906	3.912	5.204	6.840	8.896	11.456	14.618	18.493	23.040
3	0.887	1.231	1.681	2.264	3.012	3.959	5.148	6.630	8.459	10.702	13.333
3.5	0.559	0.775	1.059	1.426	1.897	2.493	3.242	4.175	5.327	6.740	8.397
4	0.374	0.519	0.709	0.955	1.271	1.670	2.172	2.797	3.569	4.515	5.625
4.5	0.263	0.365	0.498	0.671	0.892	1.173	1.525	1.964	2.506	3.171	3.951
5	0.192	0.266	0.363	0.489	0.659	0.855	1.112	1.432	1.827	2.312	2.880
5.5	0.144	0.200	0.273	0.367	0.489	0.642	0.835	1.076	1.373	1.737	2.164
6	0.111	0.154	0.210	0.283	0.376	0.495	0.644	0.829	1.057	1.338	1.667
6.5	0.087	0.121	0.165	0.223	0.296	0.389	0.506	0.652	0.832	1.052	1.311
7	0.070	0.097	0.132	0.178	0.237	0.312	0.405	0.522	0.666	0.842	1.050
7.5	0.057	0.079	0.108	0.145	0.193	0.253	0.329	0.424	0.541	0.685	0.853

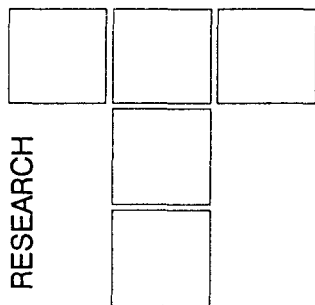
CONCLUSION

The calculated values Ψ can be used for bearing diameter $d \neq 10$ mm too, and for suitable values of H and c .

In the same way, we can find the values for Ψ for all available materials in production of porous bearings, if we have determined dependence $F=f(P)$ experimentally.

REFERENCES

- [1.] Morgan, V.T., Cameron, A.: Mechanism of lubrication in porous metal bearings, 1957 Conference of Lubrication and Wear, Institute of Mechanical Engineering, London, paper 89, pp 151-157.
- [2.] Rouleau, W.T. : Hydrodynamic lubrication of narrow press-fitted porous metal bearings, Journal of Basic Engineering, March 1963, pp. 123-128.
- [3.] Murti, P.R.K. : Hydrodynamic lubrication of short porous bearings, Wear 19 (1972), pp. 17-25.



B. TADIĆ, S. MITROVIĆ

Thin-walled Pipes Bending by Application of Friction Generated Heat

Application of friction generated heat for forming of different elements is one of the well-known methods, namely technologies, which is characterized by high economy and productivity of the process. However, according to the literature at one's disposal, the friction generated heat was not applied in operations of bending, neither thick nor thin-walled pipes.

In operations of pipes bending, that have relatively small ratio of deflection to pipe diameter, exclusively is applied heating of the critical zone by special inductors. This method of making arcs requires very high investments into the manufacturing equipment.

In this paper are presented fundamentals of the method of the friction generated heat, and the possibility is analyzed for application of such generated heat in the process of bending the copper arcs.

Besides that, in the paper is shown the idea for solution of the machine based on the presented method.

Keywords: Friction generated heat, thin-walled pipes bending, copper arcs bending

1. INTRODUCTORY CONSIDERATIONS

A pipe bending is a specific kind of bending. During the bending process pipes are subjected to forces that are deforming the original shape (section) of the pipe, so the danger exists for the pipes to lose the continuity of the section. Danger for changing the original shape exists in the critical bending zone. This is why such a place (critical zone) should be protected, as much as possible, by corresponding design measures. A very difficult type of bending is bending of thin-walled pipes, especially if they are bent to relatively small bending radii. In practice exist several developed methods and devices for straight line and circular pipes bending. However, by application of these classical methods (bending over rollers, bending with the slot link, etc.), it is not possible to perform the curvilinear bending of copper arcs in cases when the ratio of bending radius to pipe diameter is $r \leq 1.5 \cdot d$. Bending of these arcs belongs into special bending technologies that are based on heating of the critical zones by special inductive heaters. Inductive heating of critical zones requires specialized electroenergetic devices; thus making arcs according to this method is economically justified only in the batch production conditions. This method is applied for copper arcs manufacturing by the well-known French company "SUDO" that is a main supplier for our market, too.

Starting from the fact that friction between two bodies, depending on the conditions of its realization, can generate significant quantities of heat, the idea appeared that just this heat could be applied for heating the critical zones in copper arcs bending. The basic principles of heat generation by friction, and considerations related to possibility of application of that heat for heating the critical zones in bending, will be the subject of the following discussion.

2. BASIC PRINCIPLES OF HEAT GENERATION BY FRICTION

By friction between two bodies in contact, the certain amount of heat is generated, which is dependent on conditions of contact realization. If we analyze the thermal phenomena in contact between two bodies (Fig. 1), in presence of normal loading F_n and sliding speed v , we can conclude that the generated quantity of heat is a complex function of normal load F_n , sliding speed v , angle φ and many other geometrical, mechanical and thermal, namely tribological characteristics of both bodies in contact.

Analogously to the previous consideration, the thermal phenomena, which appear during the contact of pipe 1 and bush 2, can be analyzed (Figure 2).

Dr Branko Tadic, dipl. ing.,
Slobodan Mitrovic, dipl. ing.
Faculty of Mechanical Engineering, Kragujevac

This work represents the part of results of research on innovative project I.5.1753 partially financially supported by Ministry for science and technology of Republic of Serbia and partially by D.D. "Zastava-Mašine"

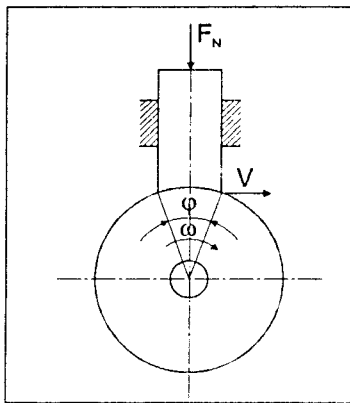


Figure 1

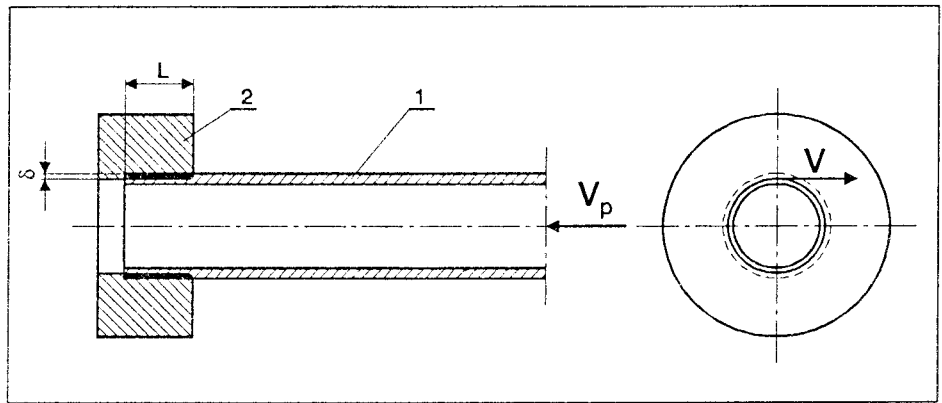


Figure 2

Namely the pipe is moving with certain velocity of auxiliary motion v_p , while the bush is rotating with peripheral velocity v . A certain overlap δ exists between the pipe and the bush.

The generated quantity of heat and intensity of the heat generation are, in this case, functions of peripheral velocity v , velocity of auxiliary motion v_p , contact length, and other tribological characteristics of pipe 1 and bush 2, what can be expressed in form of functions:

$$Q = f_1(v, v_p, \delta, L, TC, t)$$

$$I_Q = f_2(v, v_p, \delta, L, TC, t)$$

where Q - is the generated quantity of heat
 I_Q - is the heat generation intensity, and
 TC - are the other tribological characteristics of the pipe and the bush.

Definition of developed quantity of heat and heat generation intensity, as complex, non-stationary functions of conditions of contact realization, represents a very complex problem, from the theoretical viewpoint. However, from practical, engineering aspect, both generated heat quantity and heat generation intensity, can be controlled within the certain range, by some of the parameters, which are defining the contact realization conditions.

For instance, for the chosen values of overlap δ and velocity v , and other parameters, by the auxiliary motion velocity v_p , we can control functions Q and I_Q , within a very wide interval. Namely, certain needed quantity of heat we can obtain by finding one of the parameters, v , v_p , or some other, which corresponds to that quantity of heat.

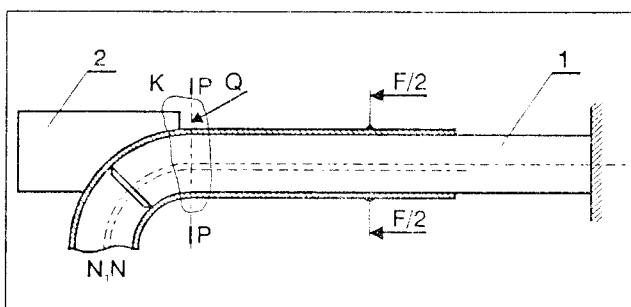


Figure 3

In engineering practice exist a large number of operations of straight line forming (contractions, expansions, etc.), that are based on the presented principle. Normally, all these operations are characterized by a series of technological details related to design of tools and equipment for forming, what is out of scope of this investigation.

3. CRITICAL ZONES HEATING DURING THE PIPES BENDING

In pipes bending, generally considered, in certain bending zone appear very complex stress and strain fields. Due to the high degree of deformation which appears when the ratio is $r \leq 1.5 \cdot d$, heating of pipes is necessary, and the heat of friction should be brought exactly into the critical bending zone.

In order to analyze the stress and strain states in the bending zone, one of possible methods of pipes bending is going to be considered, according to Figure 3. The force F according to this method pushes the pipe over the inner 1 and outer shaping tool 2. The pipe is, from the point of force action till the section $P-P$ subjected to compressive stresses over the whole cross-section. Above the neutral axis N , to the left of the section $P-P$, the pipe is subjected to tensile stresses, while below the neutral axis, to the left of the section $P-P$, it is subjected to compressive stresses. The bending area, bounded by the contour K , represents the bending zone in which the complete plastic deformation of pipe occurs. The bending zone extends also partially to the right of the section $P-P$, due to inevitable existence of clearances between the shaping tools and pipe, and due to other possible factors.

Complex stress and strain states, which due to present clearances, deviation of mechanical characteristics of pipe, etc., have also certain stochastic dimension, prevent the possibility that stresses and strains can be quantitatively expressed as functions of parameters that are defining the bending conditions. When the deformation degrees are high ($r \leq 1.5 \cdot d$), in the case of pipes bending without heating, in the compression zone will appear wrinkles on the arc. Bringing the certain heat quantity Q

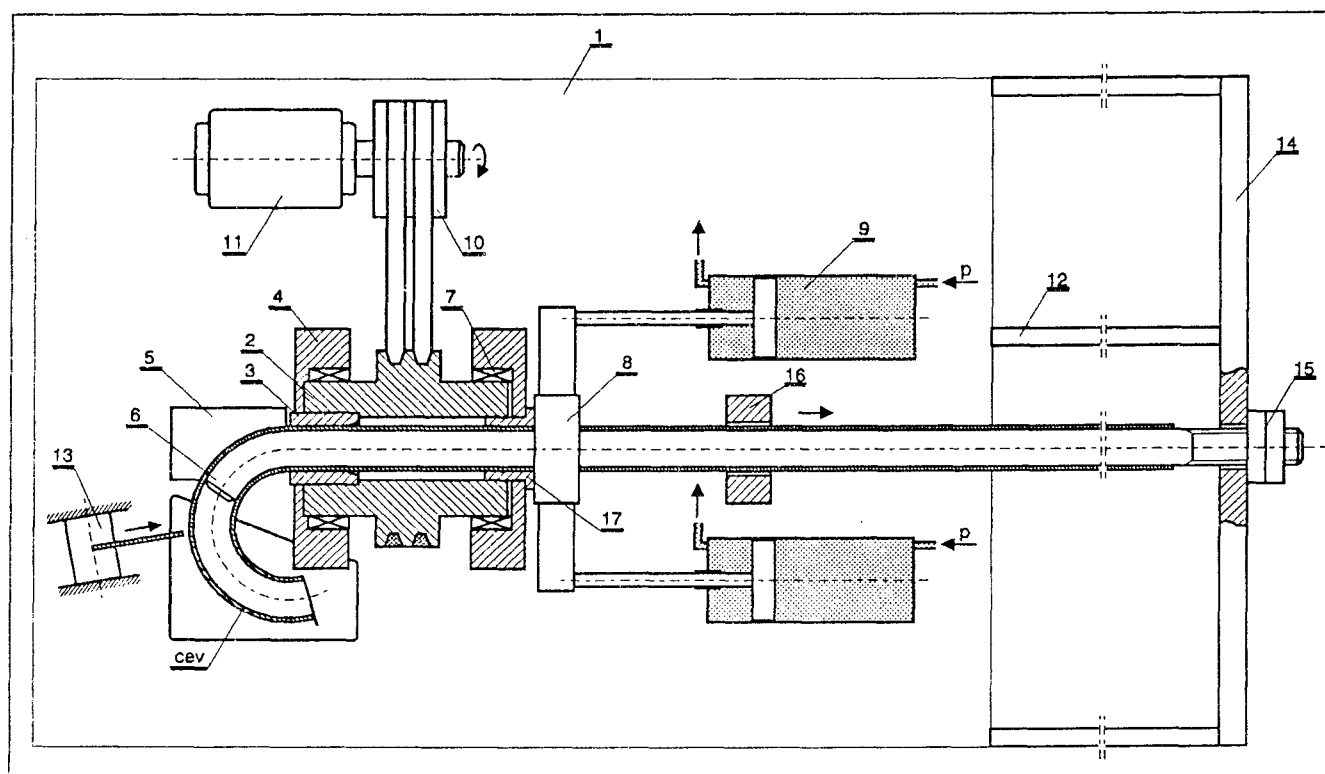


Figure 4

into the bending zone leads to decrease of mechanical characteristics of the pipe material, and to increase of the permissible degree of deformation.

4. PRESENTATION OF THE SOLUTION IDEA FOR PIPES BENDING MACHINE

The copper arcs bending procedure will here be described by use of the schematic representation of the bending machine shown in Figure 4. The pipe is placed over the inner-shaping tool 6, whose position with respect to the bush 3, is adjusted by the nuts 15. In the initial position, the pipe is by detachable connection attached to a rotating head 2, which is, by electric actuator 11 and belt transmission 10, rotating with certain number of revolutions. The rotating head 2 is placed into bearings 7, which lie in supports 4. Supports 4, electric actuator 11, pneumatic cylinders 9, limiter 16, the cutting off saw assembly 13, and outer shaping tool 5, are all placed on the main plate 1. The pipe is held by the special clamping head 8, which is connected with piston rods of pneumatic cylinders 9. Pipe pushing is done from the adjustable limiter 16 to the bush 17. Limiter 16 is adjusted along the x-axis depending on the pipe diameter and bending radius to pipe diameter ratio. Force, needed for pipe bending is obtained by the compressed air of pressure p , and the pushing velocity regulation is done by the throttling nozzles, that are placed on the outlet pipe.

The holder of the inner shaping tool 14 is, via the fixing elements 12, fixed to the main plate 1 and machine stand which is not shown on this scheme.

When the special clammer 8, that is pushing the pipe from the limiter 16, touches the bush 17 by its front face, the process of arc bending is completed. The clammer remains tight, and the cutting off saw assembly is activated. The cut arc falls through the hole in the main plate into the container that is positioned on the bottom part of the stand. After the arc cut off, the pipe is released, and the clammer is, by the pneumatic cylinders brought to the limiter 16i, into the new starting position.

The heat quantity that is brought to the bending zone can be controlled via the size of the overlap between bush 3 and pipe, and via the velocity of the bush rotation and the pipe pushing velocity. When switching to a new bending radius, i.e., to a new pipe diameter, certain parts of the machine must be changed. The variable elements are: heating bush 3, outer shaping tool 5, inner shaping tool 6, and special clammer 8 lining.

5. CONCLUSION

Based on the presented theoretical considerations and shown solution idea of the pipe-bending machine, the following conclusions can be drawn:

- The bending process of pipes with relatively small bending radius to pipe diameter ratio is characterized by the high degree of material deformation, thus it is

necessary to bring certain quantity of heat into the critical bending zone.

- Stress and strain states in the bending zone are very complex, especially when the critical zone is heated, so it is very difficult to mathematically determine the quantity and intensity of the heat needed for realization of the bending process.
- The quantity and intensity of the heat brought into the bending zone can be controlled by some of the process input parameters (sliding velocity, pipe moving velocity, etc.), what represents one of the key assumptions of the described procedure.
- According to the presented solution idea, the bending machine enables continuous regulation of the input parameters, so by monitoring the output parameters (shape of the arc, radial section sizes, etc.), is possible to practically determine the necessary quantity and intensity of heat brought into the bending zone.

It should be stressed that the pipes bending procedure according to the presented method is accompanied by a

series of problem of technical nature (selection of the heating bush to pipe overlap, lubrication system, etc.), which are not considered within the scope of this work.

REFERENCES

- [1.] *Bogojawlwnskij, K.N., Neubauer, A., Wladimirowitch, V., Technologie der Fertigung von Leichtbau-profilen*, VEB Deutscher Verlag fuer Grundstoffindustrie, Leipzig, 1985.
- [2.] *Durđanović, M., Investigation of the pipe profiles ends forming by friction*, Doctoral dissertation, Niš, 1990.
- [3.] *Protasov, V.B., O generaciji tepla pri vrešnem trenii, Trenie i iznos*, Tom II, No 1/81.
- [4.] *Imšenik, P.K., O nagreve pri svarke treniem*, Svaročnoe proizvodstvo, No 10/73.
- [5.] *Tadić, B., Nedić, B., Influence of Tribometer Constructive Solutions on Friction Force Measurements Reliability*, Journal of the Balkan Tribological Association, Vol. 4, No.1, 8-16 (1998).

I. KLIANAR, A. STEFANOVIĆ, M. RAJKOVIĆ

Possibilities of Piston-cylinder Diagnostics of Fits of Motors

RESEARCH

This paper considers the problem related to the diagnostics of piston-cylinder groups of the Internal Combustion engines. The data below were provided by concrete testing of 6 otto engines of the same type (24 piston-cylinder groups) and different technical condition. The analysis of the results achieved through the testing and the data from the relevant literature have led to the evaluation of the existing diagnostic methods and parameters and distinguished those which, from the aspects of reliability, selectivity, informative ability, sensitivity to other influences and suitability for application in workshop and exploitation conditions give greater effects in practice.

Keywords: diagnostics piston-cylinder group, Internal Combustion engine

1. INTRODUCTION

The importance of the technical diagnostics of engines is rising nowadays. It enables the optimization of the process of maintenance, greater exploiting reliability and availability, as well as the prognosis of the resource of the engine left. Special importance belongs to the technical diagnostics of piston-cylinder groups, regarding the fact that the estimation of the necessity of the general overhaul of an engine is brought mainly on the basis of the condition of this group of elements.

A great number of direct and indirect methods for the diagnostics of piston-cylinder groups have been developed so far, and for evaluation of their technical conditions, a great number of parameters are used, such as: blow-by of gases, the pressure in cylinders at the end of the compression stroke, non-hermetic properties of the cylinder, the temperature of exhaust gases, oil consumption, power of current of electrical starter motor, vibrations, external speed characteristics, characteristics of idling speed, composition of exhaust gases, etc [1].

However, a simultaneous application of all, or at least a great number of listed methods, is not rational and economical in spite of the possibility to give the most complete and accurate evaluation of the condition. Therefore, it is necessary to choose the diagnostic methods and parameters which will, from the aspect of reliability, selectivity, informative ability, sensitivity to other influences and suitability for realization in workshop and

exploitation conditions, give the greatest effects in practice. With a view to achieving this aim, this paper provides the evaluation of the existing diagnostic methods and parameters based on the analysis of the testing and on the relevant literature and distinguishes those that are with respect to the aspects mentioned, most suitable in practice.

2. DIAGNOSTIC METHODS AND PARAMETERS

The investigations of diagnostic methods and parameters performed so far have indicated that the methods for measuring oil consumption, power of current of electrical starter motor, vibrations, external speed characteristics, composition of exhaust gases and concentration of products of wear in oil, are not suitable for fast diagnostics in workshop and exploitation conditions.

The oil consumption in engines is not sufficiently reliable diagnostic parameter. It is insufficiently selective, since the oil consumption is a reflection of the state of all cylinders together, i.e. the engine as a whole. It is impossible to locate the defect with reliability, and the global estimation of the state of piston-cylinder groups can be given only if there is no leaking of the oil out of the engine. All that, as well as the necessity to perform longer testing at the engine brake, make these parameters unsuitable for diagnostics in practice [2].

A similar situation is also with the external speed characteristics of the engine [P_e , M , G_h , and g_e] which belong to the so called dependent diagnostic parameters and give only a general picture of the condition of the engine. In the diagnostics of piston-cylinder group they do not fulfill the conditions of reliability and selectivity, and their determination requires the use of the engine brake.

*Prof. Dr Ivan Klianar, dipl. ing.,
Fakultet tehničkih nauka Novi Sad,
Prof. Dr Aleksandar Stefanović, dipl. ing.,
Mašinski fakultet Niš,
Milić Rajković dipl. hem., Bell Chemicals Kikinda*

The power of current of the electrical starter motor is neither sufficiently reliable nor is it a selective diagnostic parameter. It gives relatively rough picture of the condition of the piston-cylinder group. Its application is only recommended in case of difficult access to the cylinders for measuring of the compression pressure or hermetic properties, and in case of engines with more than 4 cylinders [3].

Amplitude-frequency spectra as diagnostic parameters in measuring of vibrations, satisfy the criteria of reliability, selectivity and informative ability, but due to relatively complex and expensive equipment, which includes the use of computers, and due to necessity of working at the motor brake, they are not suitable for practical application [4].

The composition of the exhaust gases is also a dependent diagnostic parameter and represents a complex function of many influences. For the diagnostics of the piston-cylinder group it is not applied in practice due to non-reliability, non-selectivity and great sensitivity to many other influences related to characteristics of fuel-air mixture, constructive parameters and exploitation factors.

The concentration of products of wear in the oil, i.e. the estimation of the speed and quantity of accumulation of individual elements in oil, satisfies conditions in which the parameters of outlet processes can serve as symptoms of technical state of the engine. To each value of a structural parameter correspond a determined speed of wear of parts and determined regularity in the accumulation of products of wear in the oil. However, a long and complicated procedure related to taking oil sample, the subsequent analysis of the sample in specially equipped laboratories and interpretation of results with the aid of previously made diagnostic diagrams, made this method inapplicable in practice.

It is generally thought that for the evaluation of the piston-cylinder groups state of IC engines in workshop and exploitation conditions, the most suitable methods for measuring the diagnostic parameters are non-hermetic properties of the cylinder, compression pressure and blow-by of gases, and according to some authors [1], the relation of the compression pressure to the temperature of exhaust gases. Regarding the above, our investigation was limited to measuring and analysis of the four parameters listed.

2.1. Results of testing

Concrete testing was carried out on six engines type 128A.064 ("Zastava 101") with the following characteristics:

Cycle: Otto 4-stroke
Number of cylinders: 4
Compression ratio: 9.2

Cylinder diameter: 80 mm.

Piston stroke: 55 mm

Maximal power: 40.4 kW at number of revolutions: 6000 min⁻¹

Maximum moment : 77.4 Nm at number of revolutions: 3000 min⁻¹

Engines were built in into passenger vehicles which at the moment of testing, had passed the following distance in kilometers:

Engine	A	B	C	D	E	F
10 ³ km/h	7	10	70	96	110	150

That was the basis for supposition that the engines were of different technical conditions with respect to wear of piston-cylinder group. The wear was measured later. The wear of the piston-cylinder group is defined as the increase of the clearance between the piston and the cylinder, measured in the plane perpendicular to the axis of the piston shaft, and at the distance of 51+0.25 mm from the piston front (at that point the manufacturer prescribes the installation clearance of 60+10 μm and maximum permitted clearance of 150 μm).

Before testing on all the engines, the adjustments of the following were done: the distance of breaker points, the ignition timing, the clearance between electrodes of spark plug, the quantity of oil in sump, the quantity of cooling liquid, the minimum number of revolutions at idling speed, the level of fuel in float chamber of carburetor and the content of CO in exhaust gases at idling speed. The aim was to eliminate other influences upon measured parameters to the greatest extent possible and to achieve the greatest possible reliability of obtained results in relation to the state of the piston-cylinder group.

The results obtained are given in Table 1 and Figure 1. The analytical functions are determined by using the mathematical software "MATH CAD 6.0 plus":

$$p_c = 15.2323 - 0.07554 \cdot \delta \quad \text{and} \quad r^2 = 0.90767$$

$$\Delta V = -0.2947 + 0.21707 \cdot \delta \quad \text{and} \quad r^2 = 0.97237$$

$$\Delta B = -8.2769 + 0.27507 \cdot \delta \quad \text{and} \quad r^2 = 0.96239$$

$$B = -40.4155 + 1.37918 \cdot \delta \quad \text{and} \quad r^2 = 0.99284$$

$$p_c / T_i = 7.584 + 0.069 \cdot \delta - 2.96 \times 10^{-3} \cdot \delta^2 + 1.964 \cdot \delta^3$$

$$\text{and} \quad r^2 = 0.69373$$

The determination coefficient r^2 shows the high correlation between wear and parameters such as: non-hermetic properties ΔV , compression pressure p_c and blow-by B and ΔB . Functions $p_c / T_i = f(\delta)$ and $T_i = f(\delta)$ show any significant correlation.

Table 1: Result of testing

Engine	Wear [μm]		Compression pressure [bar]	Non-hermetic property [%]	Blow-by [l/min]		Temperature of exhaust gases [$^{\circ}\text{C}$]	Relation 100 bar/ $^{\circ}\text{C}$
	δ	δ	p_e	ΔV	B	ΔV	T_i	p_e/T_i
A	50	38.7	11.7	10.3	14.9	4.6	168	6.96
	30		12.7	6.3		2.0		7.59
	39		12.4	8.0		2.5		7.38
	36		12.5	7.7		2.3		7.44
B	59	48.75	11.0	11.8	25.2	7.1	201	5.47
	38		12.1	7.7		2.5		6.02
	45		11.8	9.8		3.8		5.87
	53		11.1	11.4		5.2		5.52
C	64	61.00	10.3	12.8	42.2	9.2	212	4.86
	53		11.0	11.3		5.6		5.19
	60		11.1	12.2		8.0		5.23
	67		10.4	14.1		10.1		4.91
D	65	74.50	10.4	13.6	63.8	9.8	208	5.00
	79		8.9	17.8		14.2		4.28
	75		9.3	16.2		13.1		4.47
	79		9.0	17.2		14.8		4.33
E	62	51.50	11.5	12.5	30.4	8.2	169	6.80
	43		12.4	10.0		3.7		7.34
	50		11.6	10.4		5.2		6.86
	51		11.0	11.7		5.0		6.51
F	65	62.00	10.3	13.9	45.1	9.3	228	4.52
	50		10.9	10.3		5.2		4.78
	65		10.5	13.3		10.0		4.61
	68		10.0	14.8		10.2		4.39

2.2. Evaluation of the diagnostic parameters and methods

The parameter non-hermetic properties of the cylinder ΔV is measured on the heated engine up to the temperature of the cooling liquid $T_W = 80^{\circ}\text{C}$, when the piston is in TDC (top dead center) after the compression stroke. It is expressed in % of the loss of air. It has the least value at the end of running in of the engine, during the exploitation it increases, and the limit value is considered to be the non-hermetic property of 20%, after which the overhaul of the engine is recommended.

In this particular case the non-hermetic property of the cylinder was measured by the device SUN CYLINDER LEAKAGE TESTER CLT 251/351. The measuring showed that the values of this parameter are practically proportional to the value of wear of the elements of the piston-cylinder group, which shows the regular correspondence. The parameter also enables a relatively reliable prognosis of the resource left. Deviations can appear only in the case of non-hermetic properties of the

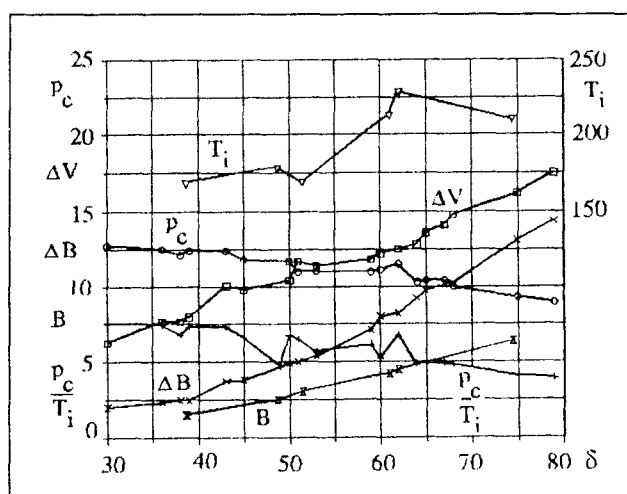


Figure 1: The influence of the cylinder wear upon diagnostic parameters

valves, a damaged sealing of the cylinder head or cracks in the cylinder head or block. Such defects are easy to detect by acoustic location of the place of air leaking,

which gives a high selectivity to the method itself. The sound at the inlet manifold indicates a non-hermetic property of the inlet valve, the sound at the exhaust manifold is a consequence of non-hermetic property of the exhaust valve. The sound at the opening for oil inlet or at the breather of the oil sump appears due to non-hermetic property of the piston-cylinder group, while bubbles on the opening of the cooler appear due to the cracks on the cylinder head or block or due to a damaged sealing between them.

Non-hermetic property of cylinders can be measured also at any position of the piston between BDC (bottom dead center) and TDC (top dead center) of the compression stroke, by which a more complete insight into condition of the overall cylinder liner is obtained. This further increases the informative ability of the parameter.

The method of measuring the non-hermetic property of the cylinder is simple for realization, the equipment needed is neither expensive nor complicated for handling. High informative ability, selectivity, reliability, insensitivity to other influences (except temperature) and defined limit value make this parameter, i.e. method, very suitable for application in workshop and exploitation conditions.

The parameter compression pressure p_c is also measured at the heated engine ($T_W = 80^\circ\text{C}$), at the number of revolutions realized by the electrical starter motor. It has the greatest value at the end of running in of the engine, after which it decreases during exploitation. According to some references [3], a limit value is defined as the drop of the compression pressure for more than 30% from the one prescribed by the factory, while according to the others the compression pressure in bars must not be lower than the value of compression ratio in a well-functioning piston-cylinder group. The overhaul is recommended in the case of difference between some cylinders of multi-cylinder engines greater than 3 bars.

The measuring done with MOTOMETER AC shows good correlation of this parameter and the value of elements wear of the piston-cylinder group. Possible deviations here are also the consequence of non-hermetic properties of other groups and parts of the cylinder working space. Such defects can be detected by repeated measurements, with the previous pouring of smaller oil quantity into the cylinder, where the increase of the compression pressure is a sign of a worn-out piston-cylinder group, and unchanged value of this parameter is an indicator of other elements non-hermetic properties. However, it is not possible to locate them precisely, i.e. to find whether the problem is in the valves, sealing, cracks in the wall or something else.

A deviation can also occur due to a different number of revolutions of the engine which can be a consequence of

the different conditions of the accumulator and electrical starter motor in each individual engine. Such deviations are also evident in measuring of pressure in cylinders of the same engine, as a consequence of the accumulator depleting. In this particular case the shortage was considerably lessened by using a special source of electric current of constant voltage (engine-starter EUROTEC EMS 280), which is also recommended in practice.

In relation to non-heretic properties of the cylinder, the parameter compression pressure is less reliable both in the diagnostics of the condition and the prognosis of the resource left (due to greater sensitivity to other influences) and it is less selective and informative. However, due to simple and fast realization and relatively cheap equipment that is used, this method is, in spite of the listed shortages, very suitable for fast diagnostics in practice.

The parameter blow-by of gases B gives an integral evaluation of the condition of all piston- cylinder groups of the engine, and by measuring at some disconnected cylinders it is also possible to obtain the condition of each and every cylinder. The numerical value of this parameter depends on the engine working regime (loading and number of revolutions), which has been confirmed by the testing we performed.

The lowest values (at the given engine working regime) are obtained after the period of running in, when the stabilization of blow-by is reached. This fact is used in case of the determination of time needed for the engine running in.

Since the parameters which can be determined on the unloaded engine are more important for the express diagnostics in workshop or exploitation conditions, the concrete measuring of gases blow-by were done on the heated engine, at idling speed of 3000 mm^{-1} . The device AVL 413/100D was used. The results indicate that the blow-by very well characterizes the wear of piston-cylinder groups of the engine as a whole. The blow-by of individual cylinders ΔB , determined as the difference of total blow-by B and blow-by at the disconnected cylinder in question, also shows a high correlation with the value of wear. Consequently, it is clear that there is also high correlation of parameters B and ΔB with parameters p_c and ΔV . The method itself is simple and can be realized very fast. The equipment needed is slightly more expensive and complicated, but still sufficiently simple for handling and application in practice. Although it is sensitive to the engine working regime, the parameter blow-by is very reliable and informative. Besides, measuring is also possible at the idling speed, which qualifies it for practical application. The basic disadvantage of the method is the lack of limit values of the parameter at the idling speed, which should be determined by a special testing on limit worn out engines. For the determination of the limit value at the normal regime there are more

recommendations, the simplest and the most acceptable being that the blow-by must not be greater than 2% of the total fresh charge. Future testing should point to the possibility of application of this recommendation in case of other regimes as well, and at the first place at idling speed. Due to a great reliability and informative ability, with simultaneous sensitivity to the working regime, the parameter blow-by is especially recommended for wider diagnostic testing in laboratory conditions (on engine brakes), not only in the sphere of maintenance, but also in the development and production of piston-cylinder groups of the engine.

The parameter temperature of exhaust gases T_i was measured at the idling speed of the engine at $n=3000 \text{ min}^{-1}$, by means of digital thermometer ISKRA DKT 1200, whose feeler was placed at the depth of 25 cm from the end of the exhausting system of the vehicle. Theoretically, with the wearing of the piston-cylinder group, due to the increase of the subsequent combustion, the temperature of the exhaust gases should be rising. However, due to high sensitivity to a set of other influences, this parameter is very unreliable, which was confirmed by the measuring described. Because of that the relation p_c/T_i , which in reference [1] was cited as a diagnostic parameter, does not show the needed reliability either. Apart from that, it is very non-selective and non-informative, and with respect to the fact that there are no concrete limit values, it is not recommended for practical application. It can be used for specific laboratory testing as an indicator of the general condition of the engine.

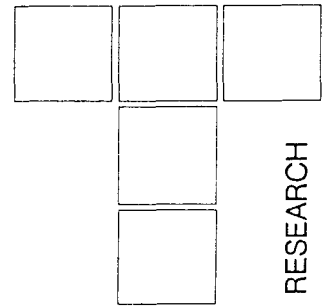
3. CONCLUSION

Based on research of the possibility to evaluate the condition of piston-cylinder groups of the engine by the application of some diagnostic methods and parameters, the following conclusions were drawn:

- From the aspect of reliability, selectivity, informative, sensitivity to other influences and suitability for realization of the measuring method, the greatest effects are achieved by the diagnostic parameters: non-hermetic properties of the cylinder, the compression pressure and gases blow-by, among which there is a very high correlation.
- For practical application in the workshop and exploitation conditions, the methods of measuring of non-hermetic properties of the cylinder and the compression pressure are recommended. The method for measuring gases blow-by is more suitable for wider diagnostic testing in laboratory conditions. For application in workshop and exploitation conditions it is recommended in the case of previously determined limit values at the measuring regime.
- Other diagnostic parameters and methods of their measuring can be used as supplementary ones, but they are not recommended for independent application.

REFERENCE

- [1.] *Mirošnikov, L.V. et al.: Diagnostirovanie tehničkog sastojanja avtomobilej na avtotransportnih pretprijatijah*, Transport, Moscow, 1977.
- [2.] *Klinar, I.: Contribution to diagnostics of piston-cylinder assembler of I.C. engines*, XVII POT Conference, Proceedings, 32-38, Novi Sad, 1992.
- [3.] *Petrović, M.: Some possibilities to determine technical state of cylinders of engines*, MVM- Proceedings 94/95, 89-97, Kragujevac, 1990.
- [4.] *Marvin, I.: Practical possibilities of vibration diagnostics of cylinders of the internal combustion engines*, MVM-Proceedings 68/69, 15-28, Kragujevac, 1986.



Research Regarding The Piston Longitudinal Profile Influence on The Displacement of The Cylinder Relative to The Cylinder Block

In this paper the results of some experimental research regarding the piston longitudinal profile influence on the displacement of the cylinder relative to the cylinder block at an overfed engine with ignition by compression are presented. To put into light the excitations that generate the cylinder vibrations a method of research based on pulses measurement was carried out. Experiments permitted us to establish the best longitudinal profile that allows the wear and friction reduction.

The piston having an optimized longitudinal profile permitted the diminuation of the cylinder vibrations as a result of the piston secondary movement when working in conditions of limit lubrication.

Keywords: Piston longitudinal profile, mono-cylinder engine, basic piston.

1. INTRODUCTION

The piston secondary movement consists of the piston lateral movement and the piston dumping. This composed movement is the result of the piston shape and mass forces due to the rod-crank mechanism. The gas pressure in the cylinder also increases this movement. The piston secondary movement has a strong negative effect on the engine working life. The results of this movement are the noise, the lubricant consumption, the loss of pressure into the cylinder, a greater wear by friction, major deformations of the piston, even piston jamming when the lubrication is at limit. The maximal reduction of the piston secondary movement can be obtained by optimizing the piston's longitudinal profile. It is necessary to ensure a minimal clearance between the cylinder and the piston to avoid jamming, that is why an exterior best profiled surface is required.

The optimized profile is desired:

- to reduce the noise and to avoid the gas loss;
- to ensure a lifting film of oil as thick as extended as it is necessary (the thickness must be as uniform as possible and the lifting area must be as limited as to avoid the mechanical losses);
- to diminish the piston thermal stress.

2. THE RESEARCH RESULTS

The target of the experiments was to determine the level of vibration when the cylinder is excited by the piston impact and the gas pressure. The tests have been carried out to find out how the piston longitudinal profile can reduce the piston secondary movement and diminish the gas loss. It is obviously known that the gas loss and the noise are the results of the piston secondary movement at the upper dead centre.

The clearance between the piston and the cylinder packs the burning chamber in the both senses of the piston's movement. The piston secondary movement is significantly influenced by the clearance between the piston and the cylinder, so the experimental tests have been carried out on the same engine, firstly equipped with a monoblock piston and secondly with a composed piston (profiled or optimized). The latter has an optimized longitudinal profile obtained by designing it accordance to spline parabolic interpolation functions. The optimized profile ensures the maximal reduction of the clearance between the piston and the cylinder. The interpolation functions permit to establish the best longitudinal profile for pieces in movement when one exactly knows a small number of points on their periphery. According to this research, optimizing the piston longitudinal profile we wished to provide the optimal distribution of the clearance between the piston and the cylinder in order to diminish the negative effects described, without affecting the engine performances. After optimizing the piston longitudinal profile we started experiments to see how this optimized profile answers to the requirements it was subjected to.

Nicolae BURNETE,
Aurica CAZILA,
Nicolae BATAGA,
Viorel Titus POP,
Technical University of Cluj-Napoca, Romania

The experimental equipment consists of the following specific instruments, according to the diagram shown in Fig. 1. To measure the cylinder displacement relative to the cylinder block, an inductive differential transducer working at a frequency of 110 Hz was used. This transducer is able to measure the cylinder oscillation amplitude at the zone where the piston changes its sense of movement. The transducer was put together with the ferromagnetic core rod that senses the cylinder displacement. The whole assembly was fixed in a tapped hole in the cylinder block. The tapped hole was placed at the zone of maximum impact of the gas pressure on the piston.

To measure the cylinder displacement three signals were simultaneously recorded:

- a) the gas pressure into the burning chamber (the signal was provided by a 6021 piezoelectric transducer with load amplifier);
- b) the cylinder displacement;
- c) a pulse signal that marked the upper dead centre (trigger).

The recordings were made using a Bruel & Kjaer 7003 tape recorder frequency modulated. The calculi showed up that the whole recording and measuring chain provides a precision up to 95%. The recordings and measurements were made for several different operating conditions. Experiments were made for several differences of temperature between the oil and the cooling agent, used for piston cooling and lubrication.

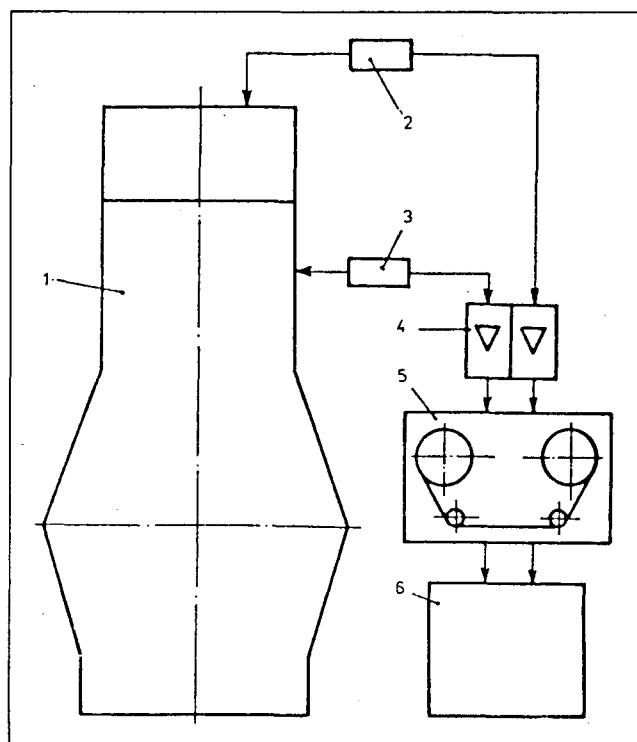


Figure 1. Experimental equipment 1. monocylinde engine;
2. pressure transducer for the burning chamber;
3. cylinder displacement transducer;
4. amplification system; 5. tape recorder
6. drawing system (oscilloscope, recorder)

The tests have been made:

- for specific conditions of the engine pre-heat;
- for specific conditions of the engine load running.

The research attempted to find out the shape modification of the piston during the experiments and the values of the engine parameters when the engine is being equipped with that kind of piston.

The measurements clearly put into light the excitations that generate the cylinder vibrations:

- the gas pressure and impact of the piston during the burning;
- the piston impact on the cylinder during the outlet stroke at $47 \div 52^\circ$ CRA (Crankshaft Angle of Rotation) before the upper dead centre;
- the piston impact on the cylinder during the inlet stroke at $100 \div 105^\circ$ CRA after the upper dead centre.

In these two positions the effect of the gases into the burning chamber is strongly diminished. It is remarkable, however, that the cylinder excitations caused only by the piston impact itself have greater values at the end of the outlet stroke than during the inlet stroke. This can be explained because the values of the outlet pressure, even diminished, are greater than the values of the overfed pressure during a great part of the operating cycle. The recordings clearly showed up that this phenomenon is the most evident in the middle zone of the balayage. In that zone the pressure variations are better transmitted when the outlet valve is closed and the inlet valve is opened, when the normal force increases.

Obviously, one can say that the recordings illustrate the cylinder displacement in the point where the transducer was located, while the normal force has a variable point of application during an operating cycle. Between the point of application of the normal force and the point where the signal is received there is a distance which diminishes the measured value relative to the real one, so that would mean an error of measurement.

According to the way how the both types of pistons fulfill their duty, we can consider that the precision of measurement is good enough. This is even more clear if one can observe that the place of the transducer is unchangeable, so the precision of measurement is the same for all tests and experiments.

The cylinder displacement, when the engine is equipped with the monoblock piston (the basic equipment), is shown in Table 1, compared with the cylinder displacement when the engine is equipped with the profiled piston.

The maximal values of the cylinder displacement when the engine is equipped with the optimized piston are $1.06 \div 2.91$ times smaller than when the engine is equip-

Table 1. The results of the cylinder displacement measurement

Operating conditions		1	2	3	4	5	6
Rotation speed rot/min		1000	1670	1790	950	1650	1800
Brake reading (F)		N	0	0	0	485	262
$\Delta t_{\text{water-oil}}, ^\circ\text{C}$		30	30	30	25	30	30
Displacement before the upper dead centre (δ_1), mm	Basic piston	0.0050	0.017	0.015	0.002	0.017	0.017
	Profiled piston	0.0031	0.010	0.0018	0	0.011	0.016
Displacement after the upper dead centre (δ_2), mm	Basic piston	0.0035	0.011	0.012	0.003	0.011	0.011
	Profiled piston	0.0012	0.0075	0.0083	0	0.0057	0.0074

Table 2. Cylinder displacement reduction when the engine is equipped with the profiled piston

Operating conditions	Cylinder displacement mm				The reduction of δ_1 displacement, mm	The reduction of δ_2 displacement, mm
	δ_1		δ_2			
	Basic piston	Profiled piston	Basic piston	Profiled piston		
2	0.005	0.0031	0.0035	0.0012	1.61	2.91
3	0.017	0.010	0.011	0.0075	1.70	1.46
6	0.017	0.011	0.011	0.0057	1.54	1.92
7	0.017	0.016	0.011	0.0074	1.06	1.48

ped with the basic monoblock piston, at the same operating conditions and the same difference of temperature between the lubricant and the cooling agent (shown in Table 2).

Generally, the cylinder displacement when the engine is equipped with the profiled piston is 22% lower in any operating conditions. When the engine is equipped with the basic piston the displacement of the cylinder takes values between a minimal value (0.0015-0.003 mm when the normal force $F=0$ and the rotation speed is $n=850-950 \text{ rot/min}$) and a maximal value (0.017-0.018 mm, when $F=117-125 \text{ N}$ and $n=1650-1800 \text{ rot/min}$). When the engine is equipped with the profiled piston the values are much diminished, between a maximal value of 0.01 mm and a minimal value of 0.0012 mm, in the same operating conditions and the same differences of temperature between the lubricant and the cooling agent. In many cases,

when using the profiled piston, the values of the displacement are 0 or nearly 0.

In Figure 2 there are shown the values of the displacement when the engine is working with the basic piston compared with the values of the displacement when the engine is working with the profiled piston, in the same operating conditions.

The cylinder vibrations take place within their own fundamental frequency, however there are some vibrations at higher frequencies, but much reduced (2-3 μm).

Comparing the vibrations in no-load running condition with the vibrations in load running conditions, when the engine is equipped with the profiled piston, one can see the significant reduction of the vibrations amplitude. This can be seen at any rotation speed.

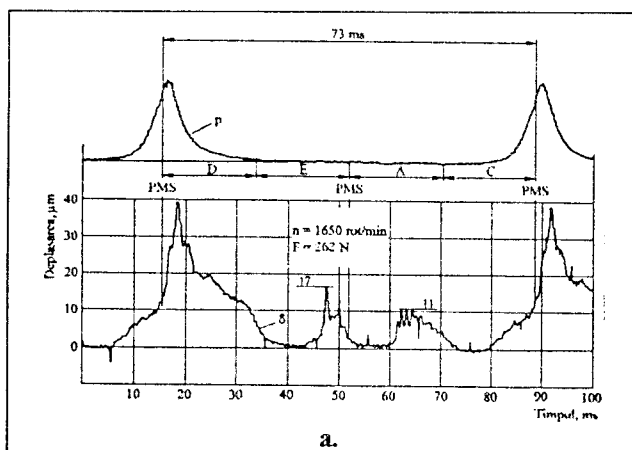


Figure 2a. Cylinder displacement when the engine is equipped with the basic piston

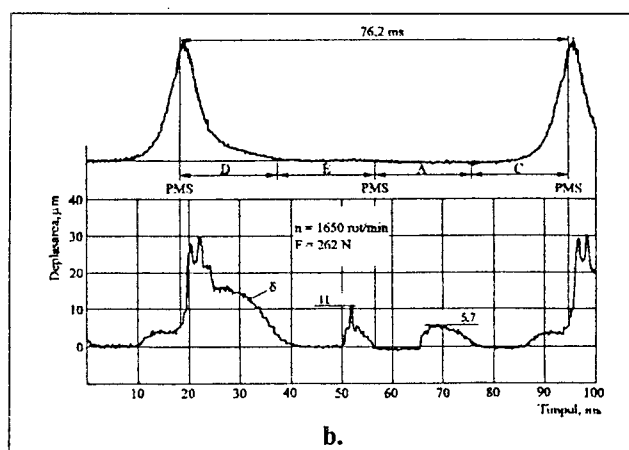


Figure 2b. Cylinder displacement when the engine is equipped with the profiled piston

These results can be also observed when one compares the level of vibrations for the cold profiled piston (at the start of the test) and the level of vibrations for the hot profiled piston (after a few minutes of work).

3. CONCLUSIONS

The experimental measurements permitted us to study the influence of the piston longitudinal profile on the vibrations generated by the piston impact with the cylinder. The vibrations of the cylinder are much reduced when the engine is equipped with the profiled piston, in any operating conditions.

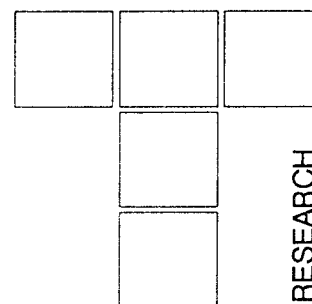
This can be done because the composed profile designed according to the spline parabolic interpolation functions

provides a minimal clearance between the cylinder and the piston, taking into account:

- the roughness of the piston and of the cylinder;
- the necessity to ensure a film of oil able to provide the hydrodynamic lubrication.

REFERENCES

- [1.] *Bataga, N., Burnete, N., Cazila, A.: Internal Combustion Engines*, EDP, Bucuresti, 1995
- [2.] *Grunwald, B.: The Theory, the Calculi and the Construction of Road Vehicles Engines*, EDP, Bucuresti, 1980
- [3.] *Tschoke, H., Essers, U., Einfluss des Zylinderdruckverlaufes auf die Sekundarbewegung des Kolbens*, in *MTZ*, Bundesrepublik Deutschland, 43, Nr. 4, 1982, pp. 157-160



I. MUSCA

Lubricant Compressibility - Theoretical and Experimental Aspects

The paper presents experimental results of compressibility for Romanian produced oils, until 1.4 GPa, correlated with theoretical results based on simple liquids theory of Diaconescu. Some observations about the solid and liquid state of oils under pressure are presented too.

Keywords: Tribology, compressibility.

1. INTRODUCTION

Compressibility behavior is a very important characteristics of fluids working in high pressure conditions. Experiments, [1], [2], showed that once the pressure increases, the relative volume occupied by the fluid reduces. This dependence passes, at a characteristic value of pressure and for some oils, from a rapid curvilinear variation to a slower slope-approximately linear one. This change indicates internal transformation in molecular position distribution.

In elastohydrodynamic (EHD) conditions, the effect of this behavior of lubricants, reflects first on the film thickness and the influence of physical feature changes on the lubricant behavior. Jacobson, [1], reveals that the lubricants which show a higher compressibility will form thinner EHD films and the minimum film thickness could appear in the central zone of the contact.

Based on experimental results, many researchers such as Jacobson, [1], Dowson, Trachmann, Fein, Goldman, [5], Ramesh, [4], etc., attempted to model the compression behavior. These researches propose many formulae which correlate the pressure with relative volume changes, but no correlation with molecular form, distribution and interactions in liquids was made.

A particular theory, for simple molecular liquids, was developed by Diaconescu, [3], and applied for similarly EHD conditions. Theoretical arguments show that in the simple molecular liquids, with spherical molecules in Wan deer Waals interactions, the increase of pressure involves a intermolecular distance reduction and a holes elimination process. These effects have different impor-

tance depending on pressure value. At lower values of pressure, intermolecular distance reductions have a small effect upon volume changing and the most important is the process of holes elimination. The holes elimination speed reduces with the increase of pressure value. Theoretical calculations show that holes density, at pressure higher than 0.5 GPa and for usual value of molecular parameters is smaller than 1%, (figure 1). So, in conditions of high pressure values (such as EHD contacts) the holes elimination process is finished and volume variations under pressure are determined principally by intermolecular distance reduction. For this solid-like behavior Diaconescu, [3], established a correlation between intermolecular distance, r_p , pressure, p , and molecular parameters for a very compact structure:

$$2 \cdot \left(\frac{\sigma}{r_p} \right)^{15} - \left(\frac{\sigma}{r_p} \right)^9 = \frac{\sqrt{2}}{96} \cdot p \cdot \frac{\sigma^3}{\epsilon} \quad (1)$$

The holes density, d_p , in liquid states, is given by a Bose-Einstein distribution:

$$d_p = \frac{n_p}{N} = \frac{1}{\exp \left(\frac{\Delta g_l(p)}{kT} \right) - 1} \quad (2)$$

The relative volume variation of a mole of substance, given only by holes elimination from zero to p values of pressure, can be written as:

$$\frac{\Delta v_g}{v_0} = \frac{d_0 - d_p}{1 + d_0} \cdot \left(\frac{r_p}{r_0} \right)^3 \quad (3)$$

An example of pressure dependence of this reduction is presented in figure 2.

Ilie MUSCA

"Stefan cel Mare" University, Suceava, Romania

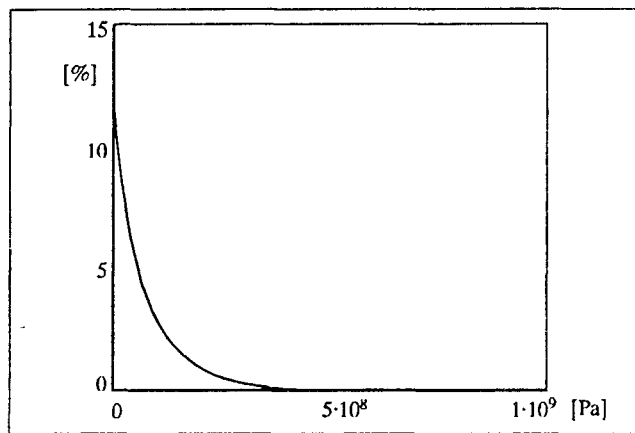


Fig. 1. Holes density-pressure correlations, ($\sigma=5.314 \cdot 10^{-10}$, $\epsilon/k=313^\circ\text{K}$)

2. THEORETICAL CONSIDERATIONS

a. Liquid without vacancies. In high pressure conditions, so no vacancies are present in fluid, intermolecular equilibrium distance, r_p , is correlated with pressure by a relation:

$$p = \frac{A}{r^{15}} - \frac{B}{r^9} \quad (4)$$

where A and B are material's constants.

At zero pressure value, a direct correlation between A and B can be obtained as:

$$A = B \cdot r_0^6 \quad (5)$$

and equation (4) can be rewritten as:

$$p = B \cdot \left(\frac{r_0^6}{r_p^{15}} - \frac{1}{r_p^9} \right) \quad (6)$$

The volume affected for a molecule in fluid is directly proportional to on the cube power of the intermolecular distance:

$$v = \text{const} : r^3 \quad (7)$$

and from intermolecular distance-pressure correlation, a correlation can be deduced of molecule volume with pressure:

$$p = B_1 \cdot \left(\frac{v_0^2}{v_p^5} - \frac{1}{v_p^3} \right) \quad (8)$$

or

$$p = \frac{B_1}{v_0^2} \cdot \left(\frac{1}{(1-x)^5} - \frac{1}{(1-x)^3} \right) \quad (9)$$

where

$$x = \frac{v_0 - v_p}{v_0} \quad (10)$$

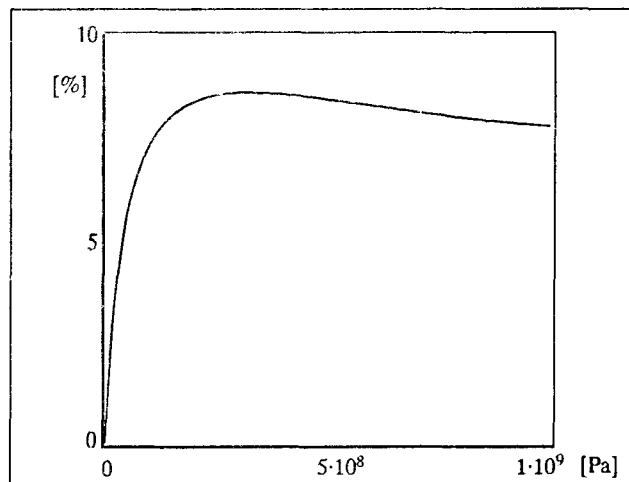


Fig. 2. Relative volume reduction under pressure by holes elimination ($\sigma=5.314 \cdot 10^{-10}$, $\epsilon/k=313^\circ\text{K}$)

An experimental value for x , can be used to determine value of constant B_1 . This equation (9) can be used to approximate the pressure-volume correlation for lubricants.

b. Vacancies presence in liquids affects the compressibility in range of lower pressure values. A theoretical correlation of relative volume reduction in presence and absence of holes in liquid is presented in figure 3, [6]. We can see that only at lower pressure values the difference between two curves has an important variation.

At high pressure the two curves are similar and, in this range, compression curve including vacancies effects can be approximated by no vacancies compression curve:

$$\left(\frac{\Delta v}{v_0} \right)_{\text{real}} = \left(\frac{\Delta v}{v_0} \right)_{\text{no holes liquid}} + k_x \quad (11)$$

or

$$1 + \frac{r_p^3 \cdot (d_p + 1)}{r_0^3 \cdot (d_0 + 1)} = 1 - \frac{r_p^3}{r_0^3} + k_x \quad (12)$$

and k_x a constant value depending of initial hole density.

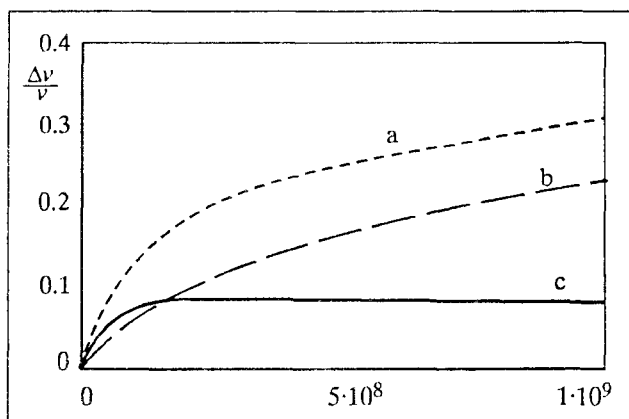


Fig. 3. Relative volume-pressure theoretical correlation; a - liquid without holes, b - liquid with holes, c - difference between b and a, ($\sigma = 5.314 \cdot 10^{-10}$, $\epsilon/k = 313^\circ\text{K}$)

In the experimental values of relative reduced volume, the effect of hole elimination is included too, but the pressure-volume correlation is written at high pressure, so a correlation such as

$$x \rightarrow x_{no \text{ holes}} - \left(\frac{\Delta v}{v_0} \right)_{holes} \quad (13)$$

is imperative.

The relative volume reduction by hole elimination is depending on pressure value. We accept for this dependence the correlation:

$$\left(\frac{\Delta v}{v_0} \right)_{holes} = d_0 \cdot [1 - \exp(\alpha p)] \quad (14)$$

where d_0 is holes density at zero pressure and α a constant parameter.

With this assumption, from (9) can be derived a new formula:

$$p = \frac{B_1'}{v_0^2} \cdot \left[\frac{1}{(1-x+d_0[1-\exp(\alpha p)])^5} - \frac{1}{(1-x+d_0[1-\exp(\alpha p)])^3} \right] \quad (15)$$

Expressions (9) and (15) are two new formulae for fluids compression behavior modelling.

3. COMPRESSION EXPERIMENTS

A classical compression test rig working until 1.4 GPa was used for oils testing. Two typical behaviors of oils under pressure were detected:

1. When pressure increases, the volume reduction increases continuously and no local change in curve's slope was detected. In these situations it is assumed that no solid-liquid state transformation occurs.
2. For some liquids, important changes of curve's slope were detected at a critical value of pressure and they were associated with liquid-solid state transition, similar to Ohno, [9].

4. THEORY-EXPERIMENT CORRELATION

From experiments for two Romanian produced oils (T90EP2 and M30 Super) the values for constants in proposed formulae were calculated. These values are presented in the table 1.

Theoretical and semi-empirical correlation of relative volume with pressure are plotted in figures 4 and 5.

Table 1. Approximate values for coefficients

	B_1/v_0	B_1'/v_0	d_0	a
M30Super	1.806	10.794	0.11	2.53
T90EP2	0.700	1.541	0.11	0.888

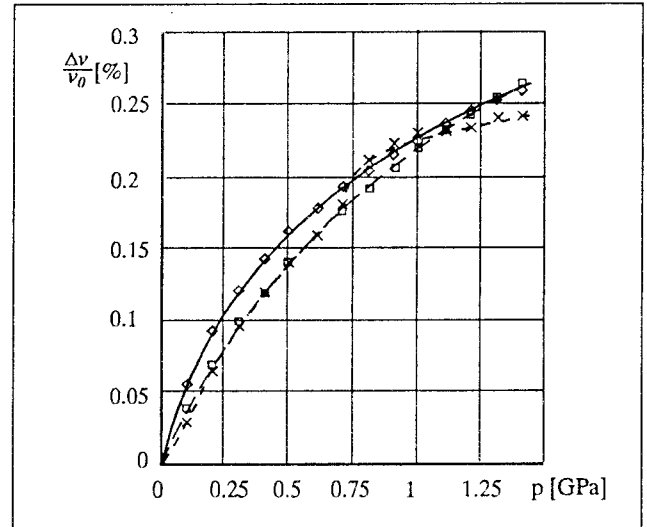


Fig. 4. Theoretical and semi-empirical correlation for T90EP2 romanian oil. \diamond - formula (9), \square - formula (15), \times - experimental

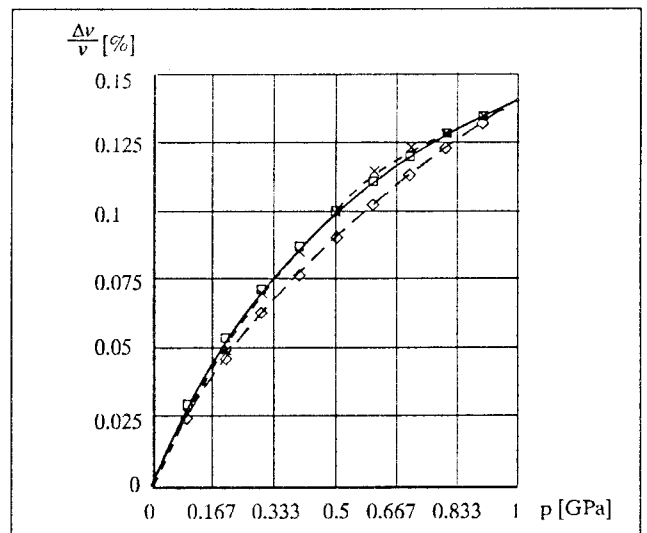


Fig. 5. Theoretical and semi-empirical correlation for M30 romanian oil. \diamond - formula (9), \square - formula (15), \times - experimental

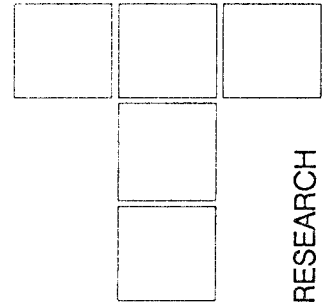
CONCLUSION

- The two formulae (9 and 15) give a good correlation theory-experiment. More accuracy is offered by the second formula.
- For T90EP2 oil the changes of curve's slope detected experimentally show a different behavior under pressure and no good precision of approximation can be obtained over experiment pressure range.

REFERENCES

- [1.] *Jacobson, Bo., Vinet, P.A., Model for the Influence of Pressure on the Bulk Modulus and the Influence of Temperature on the Solidification Pressure of Liquids Lubricants.* ASME Journ. of Lubr. Tech., Vol.109,1987, 709-713.
- [2.] *Ramesh, K.T., The Short-Time Compressibility of Elastohydrodynamic Lubricants,* ASME Journ. of Trib.,1991, Vol.113, 361-371.
- [3.] *Diaconescu, E.N., The Effect of Pressure Upon Solid-like Shear Properties of Molecular Liquids - A Physical Point of View,* Acta Tribologica, Vol.1, 1,1992, 49-62.
- [4.] *Ramesh, K.T., Clifton, R.I., A Pressures Shear Plate Impact Experiment for Studying of Lubricants at High Pressures and High Shearing Rates,* ASME Journ. of Trib.,1987, Vol. 109, 215- 222.
- [5.] *Goldman, I.B., Venkatesan, F.S., The Compressibility of Selected Fluids at Pressures up to 230 000 PSI,* Lubrication Engineering, 1971, 334- 341.
- [6.] *Musca, I., Rheological Implication in EHD Lubrication,* Ph.D. Thesis, Suceava 1996, 238p, (in Romanian).
- [7.] *I. Musca, I., Diaconescu, E.N., Aspecte Privind Comportarea Fluidelor la Comprimate, VAREHD 7,* Suceava,1994.
- [8.] *Musca, I., About Lubricant Compressibility,* EUROTRIB'93, Budapest, 92-97.
- [9.] *Ohno, N., at al., Diagram for Estimation of the Solidified Film Thickness in High Pressure EHD Contacts,* 1994, Leeds-Lyon Symp.

Friction Influence on The Uniformity Deformation Coefficient in The Cold Forming Ball Bearing Semi-cages



The paper presents the influence of friction on the uniformity deformation coefficient in the corrugating with stretching operation of the plane workpieces for semi-cages in ball-bearing processing. This influence was determined using a mathematical model calculus and was verified with an experimental model based on corrugated samples with profile stretching with varying roughness, lubricated and unlubricated.

Knowing the friction influence on the uniformity deformation, the dimensioning phase of the circular crowns for a certain manufacturing program is carried out on a computer. The internal diameter of a circular crown will be equal to the external diameter of the circular crown of a semi-cage used for another bearing size from the manufacturing program.

Thus, the semi-cage cold forming technology is carried out with small material waste, with a good influence on the production material expenses.

Keywords: Ball bearing semi-cage, friction, uniformity deformation coefficient.

1. INTRODUCTION

The sheet metal cold forming technologies for radial ball-bearing semi-cages exist in variants from strip or individual workpieces.

The technological variant adopted is determined as function of the semi-cages dimensions (fig. 1), the processing program, the endowment with technological equipment for cold forming, based on the technical-economic calculus [1]. The main processing operations frequently used in these technologies are: cutting, punching, corrugation, calibration, burring and polishing.

The corrugating operation for the circular crown decreases the crown's dimensions contained in its plane and to obtain the appropriate values for the finite piece (fig. 2).

The used material coefficient in processing this group of pieces is very low as compared to other elements from ball-bearing construction, this ranging between 19.5% and 23%.

If we consider the corrugating operation done with tangential stretching and the middle specific elongation ϵ_m , the plane circular crown for semi-cage processing will have the middle diameter D_M , established by the relation:

$$D_M = \frac{D_{MO}}{1 + \epsilon_m} \quad (1)$$

The diameter D_{MO} can be calculated as a function of the dimensions of semi-cages [2], and the other dimensions for the plane circular crown by the relations:

$$\begin{aligned} D_e &= \left(D_M + \frac{b}{1 - \nu_p \cdot \epsilon_m} \right)^{+a_{se}} \\ D_i &= \left(D_M - \frac{b}{1 - \nu_p \cdot \epsilon_m} \right)^{+a_{si}} \end{aligned} \quad (2)$$

where:

$b = \frac{d_e - d_i}{2}$ is the plane circular crown width;

d_e, d_i - the external and internal diameter of the semi-cage, respectively;

$a_{se}, a_{ie}, a_{si}, a_{ii}$ - the upper respective interior deviations for the dimension of the plane circular crown ($a_{se} = -a_{ii}$; $a_{ie} = -a_{si}$);

$\nu_p = 0.5$ - the Poisson coefficient for the plastic deformation.

Lecturer Dr. Eng. Lucian V. SEVERIN
"Stefan cel Mare" University of Suceava,
Professor Dr. Eng. Mihai Al. TEODORESCU
"Dunarea de Jos" University of Galatzi,
Lecturer Dr. Eng. Dumitru AMARANDEI
"Stefan cel Mare" University of Suceava

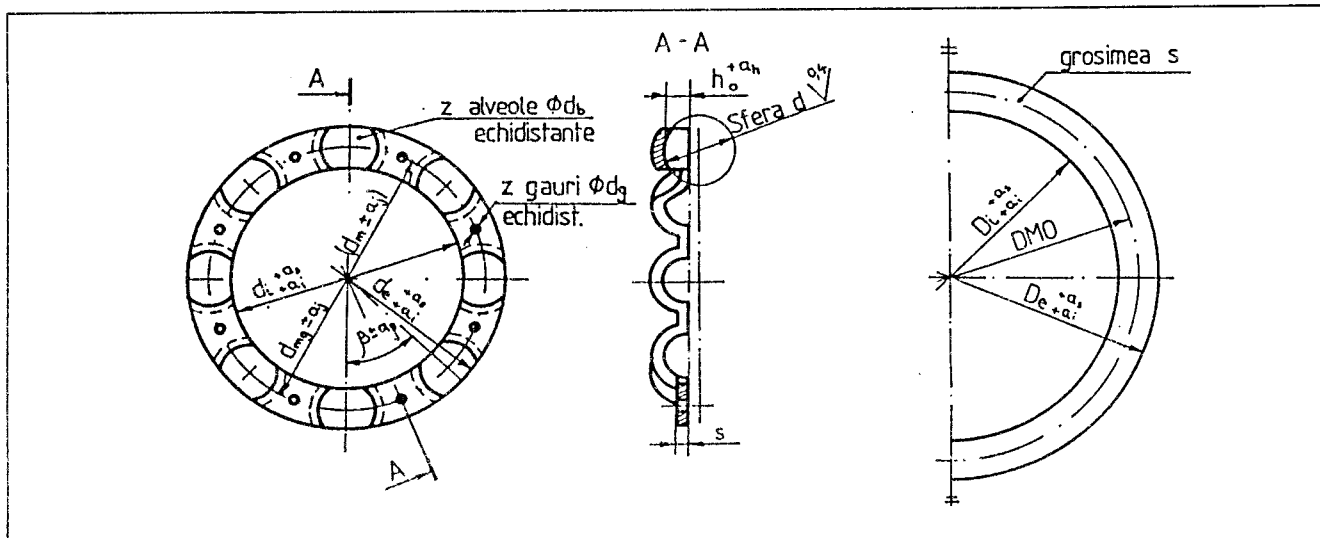


Fig. 1

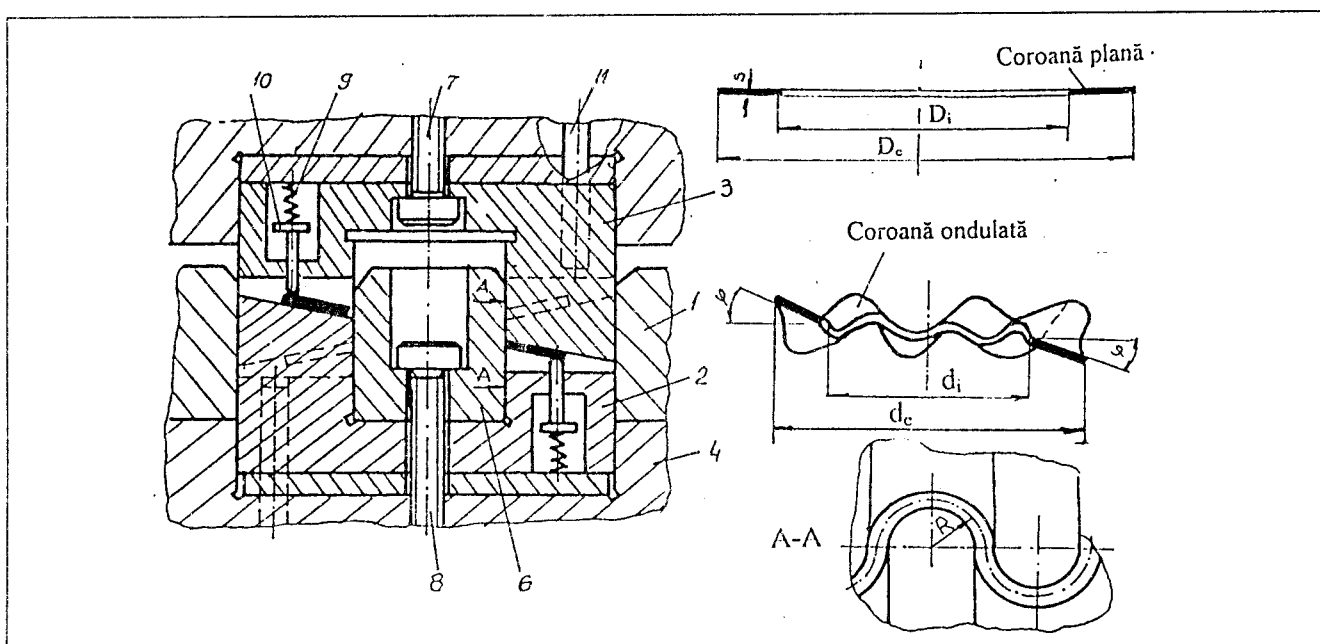


Fig. 2

If the domain in which the middle specific elongation ε_m can take values is known, the calculus of the semi-cage dimensions can be done for a certain manufacturing program, so that the waste dimensions obtained at stamping the sheet metal disc for a plane circular crown to coincide with the external diameter of the plane circular crown for processing the other semi-cage dimension from the manufacturing program (fig. 3). The obtained semi-cages will have the thickness sensibly different according to the deformation value applied, thickness that can be determined by relation:

$$s_i = s \cdot (1 - \varepsilon_{mi}) \quad (3)$$

Thus, more ball-bearings' semi-cages can be processed from that same sheet metal surface and the efficiency material coefficient in processing increases.

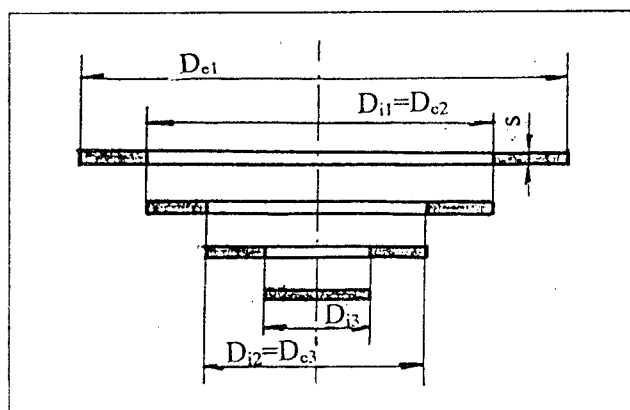


Fig. 3

2. DETERMINATION OF THE MIDDLE SPECIFIC ELONGATION AT COLD CORRUGATING WITH STRETCHING FOR CIRCULAR CROWN PROCESSING

The middle specific elongation value, ε_m , varies at the cold corrugating process in the interval $[\varepsilon_{min}, \varepsilon_{max}]$. Because it is necessary to achieve plastic deformation through the material thickness of the workpiece and to limit the spring action, the value of ε_{min} is 3-5% [3]. The value of ε_{max} can be estimated by the relation:

$$\varepsilon_{max} = \varepsilon_a = \xi \cdot k_e \cdot \eta \cdot \varepsilon_r \quad (4)$$

where: ε_r is the material standard fracture specific elongation of the plane circular crown, determined according to material;
 η - the used material plasticity coefficient in corrugating operation;
 ξ - the coefficient that emphasizes the corrugating conditions influence on the middle specific elongation;
 k_e - coefficient that takes into account the material plasticity decrease due to material cutting at stamping die.

If we take into account that, for a certain material and technology for plane circular crown, k_e , η and ε_r do not depend on the corrugating conditions, then:

$$\varepsilon_a = k_e \cdot \eta \cdot \varepsilon_r \quad (5)$$

where ε_a is the admissible specific material elongation in the area between the corrugating profiles that it is not in contact with them (fig. 4), or:

$$\varepsilon_{ma} = \xi \cdot \varepsilon_a \quad (6)$$

For the brands of metal used in semi-cages' ball-bearings processing (A1, A2, A3 STAS 9485), the maximum value of the used material plasticity coefficient in corrugating operation, for a uniform deforming, is $\eta_{max}=0.72-0.82$. The value of the coefficient that takes into account the material plasticity decrease, due to material cutting at stamping dies, is $k_{emax}=0.75-0.8$. These values are accepted at stamping with maximum accepted interstice, that has the cutting interstice coefficient $m=0.25-0.30$ [1].

The state of stress and stretching of the material in the corrugating process is identical for these "z" corrugations. Therefore, it is enough to perform the ε_m calculation for one corrugation only.

For this calculation, a theoretical deformation model of a flexible strip among three cylinders with radius R is suggested. The strip thickness is considered as significant in comparison with other dimensions, (fig. 4).

The middle specific elongation calculation will take into account that the length L_1 of the material strip is deformed without contact with the deformation profiles and the lengths L_c are deformed by friction, with the friction

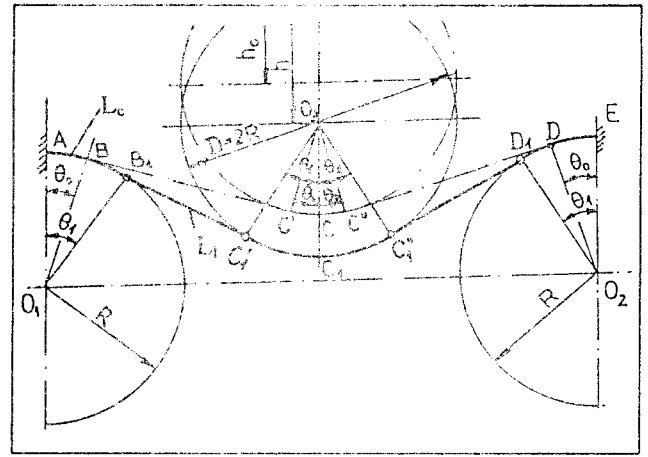


Fig. 4

coefficient μ between the material strip and the corrugating profiles, thus:

$$\varepsilon_m = \frac{2 \cdot (\Delta L_c + \Delta L_1)}{L_0} \quad (7)$$

where: ΔL_c is the strip size in contact with half of the corrugating profile;
 ΔL_1 - the strip size between the corrugating profiles;
 L_0 - the initial strip size corrugated without stretching between the profiles.

The value ΔL_c is calculated by relation [4]:

$$\Delta L_c = \int_0^{L_0} \varepsilon \cdot dL = \int_0^{\theta_0} \varepsilon \cdot R \cdot d\theta \quad (8)$$

Taking into account the relation between the stress applied at the ends of the part of the strip, which is wrapped up on a cylinder [5], and the real material characteristic, $\sigma_{real} = f(\varepsilon)$, yields:

$$\varepsilon = \varepsilon_1 \cdot e^{-\mu(\theta_0 - \theta)} \quad (9)$$

where: θ_0 is the initial wrapping up angle of the strip on the profile;
 θ - the current wrapping up angle, $\theta \in [0, \theta_0]$;
 ε_1 - the specific elongation of the value L_1 .

By substitution of (9) in (8) and performing the calculation it obtains:

$$\Delta L_c = \frac{R}{\mu} \cdot (1 - \varepsilon_1 \cdot e^{-\mu\theta_0}) \quad (10)$$

Because ε_1 is considered uniform, the elongation between profiles, ΔL_1 , it is calculated by the relation:

$$\Delta L_1 = L_1 \cdot \varepsilon_1 \quad (11)$$

L_1 can be determined from the geometrical conditions by relation:

$$L_1 = 2 \cdot R \cdot \left(\frac{\nu_0 + \cos \theta_0}{\sin \theta_0} \right) \quad (12)$$

where:

$$\theta_0 = \arcsin \frac{(1+\alpha) + (\gamma_0 - 1) \cdot \sqrt{(\gamma_0 - 1)^2 + (1+\alpha)^2} - 1}{(\gamma_0 - 1)^2 + (1+\alpha)^2};$$

$$\gamma_0 = \frac{h_0}{2R}; \quad \alpha = \frac{a}{2R}; \quad v_0 = \frac{h_0}{2R} - 1;$$

and the symbols are according to figure 4.

Also, from the geometrical conditions L_0 can be determined by expression:

$$L_0 = 4 \cdot R \cdot \left(\frac{v_0 + \cos \theta_0}{\sin \theta_0} + \theta_0 \right) \quad (13)$$

Substituting (13), (12), (11) and (10) in (7), it yields:

$$\varepsilon_m = \frac{\varepsilon_1}{\mu} \cdot \left[\frac{(1 - e^{-\mu \cdot \theta_0}) \cdot \sin \theta_0 + \mu (v_0 + \cos \theta_0)}{v_0 + \theta_0 \cdot \sin \theta_0 + \cos \theta_0} \right] \quad (14)$$

The relation (14) defines the connection between ε_m and the parameters that express the corrugation conditions when the material deformation between the corrugation profiles has the specific elongation ε_1 .

If the strip is corrugated with stretching until $\varepsilon_1 = \varepsilon_a$, then $\varepsilon_m = \varepsilon_{max}$, and the relation (14) becomes:

$$\varepsilon_{ma} = \frac{\varepsilon_a}{\mu} \cdot \left[\frac{(1 - e^{-\mu \cdot \theta_0}) \cdot \sin \theta_0 + \mu (v_0 + \cos \theta_0)}{v_0 + \theta_0 \cdot \sin \theta_0 + \cos \theta_0} \right] \quad (15)$$

If we write:

$$\xi = \frac{1}{\mu} \cdot \left[\frac{(1 - e^{-\mu \cdot \theta_0}) \cdot \sin \theta_0 + \mu (v_0 + \cos \theta_0)}{v_0 + \theta_0 \cdot \sin \theta_0 + \cos \theta_0} \right] \quad (16)$$

the relation (15) takes the form of the relation (6).

The value of ξ defined by relation (16) characterizes the influence of the corrugating with stretching conditions on the uniformity deformation and it is not influenced by the mechanical characteristics of material.

3. EXPERIMENTAL DETERMINATIONS CONCERNING THE INFLUENCE OF THE FRICTION CONDITIONS ON UNIFORMITY DEFORMATION COEFFICIENT.

The experimental results concerning the influence of the corrugation conditions on the uniformity deformation coefficient, ξ , were drawn on sheet metal samples, mark A3 K03 STAS 9485 with a width $b_0 = 6 \text{ mm}$, and a thickness $s = 1 \text{ mm}$, on a stand and with the methodology presented in [1]. The graphical representation of these results is presented in the figures 5, 6, 7 and 8.

Those were obtained on samples corrugated with stretching on profiles with different roughness, lubricated

and unlubricated, for different profile relative displacements and different initial relative corrugating amplitude.

The curve's analysis from the figure 5 emphasizes the fact that for the growth of the initial wrapping up angle of the strip on the profile, θ_0 , (or the growth of the initial relative amplitude corrugating, γ_0), the uniformity deformation coefficient decreases to certain minimum values due to the increase of the friction deformed length all along the deformed strip at one corrugation; afterwards, it starts growing again.

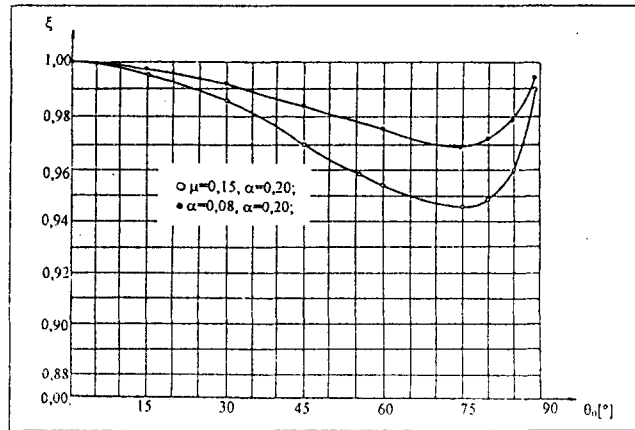


Fig. 5

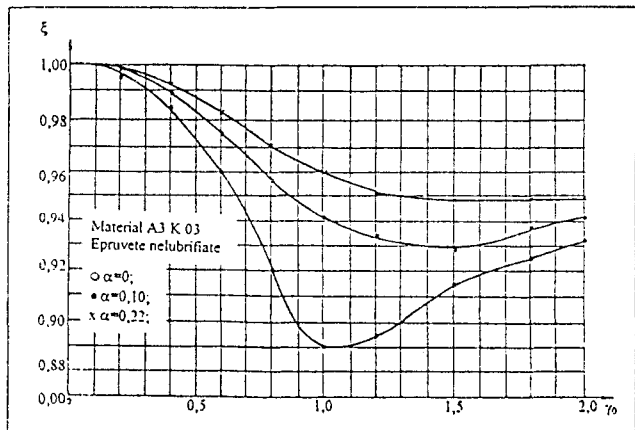


Fig. 6

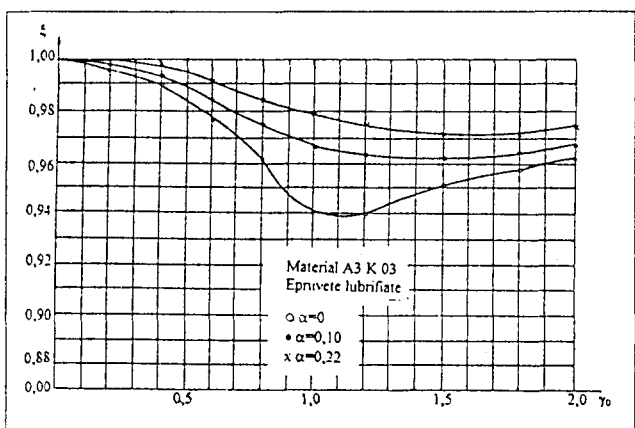


Fig. 7

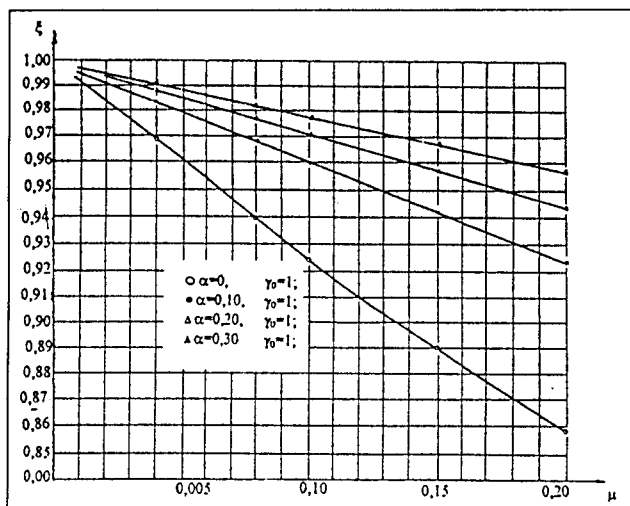


Fig. 8

The influence of lubrication function by γ_0 , and μ on the uniformity deformation coefficient, results from figures 6, 7, and 8.

Thus, the values of the coefficient ξ decreases with the growth of the relative displacement coefficient of the corrugating profiles (α) and with the growth of the friction coefficient between the strip and the corrugating profiles (μ). The least value for ξ ($\xi_{min}=0.89$) is obtained at the corrugating with stretching carried out with the unmoved profiles ($\alpha=0$), the relative amplitude corrugating $\gamma_0=1$ and without lubricant between the strip and the corrugating profiles ($\mu=0.15$).

Important values of the uniformity deformation coefficient have been obtained using the lubricated strip in deformation with the least wrapping up angle.

The results obtained with the experimental model, correspond well enough with those calculated by the relation (18).

4. CONCLUSIONS

By determining the maximum admissible values for the middle specific elongation on corrugation, ϵ_{max} , we find out the limits of the interval where that can take values, at corrugating processing with stretching of the circular crown for semi-cage's ball-bearings processing.

By processing the circular crown with different degrees of deformation, for a certain manufacturing program, the dimensioning phase is carried out with the computer in such a way that the internal diameter of a circular crown should be equal to the external diameter of circular crown for a semi-cage used for another bearing size from the manufacturing program.

Thus, the semi-cages cold working technology is carried out with small material waste and with a good influence on the production's material expenses.

REFERENCES

- [1.] Severin V. Lucian, Cercetari privind deformarea plastica la rece a coroanelor circulare cu aplicatii in constructia rulmentilor. Teza de doctorat. Universitatea "Dunarea de Jos" Galati, 1996.
- [2.] Severin V. Lucian, Teodorescu Al. Mihai, Calculation of the plane circular rim workpieces for the cold-working of the semi-cages of the radial ball bearings. Journal of Plastic Deformation, vol. 2 (1995), Nr. 1 (3). Centrul de studii si cercetari pentru deformari plastice si Universitatea "Lucian Blaga" Sibiu, 1995.
- [3.] Romanovski V., P., Stantarea si matritarea la rece. Editura tehnica, Bucuresti, 1970
- [4.] Ponomarev, S., D., s. a., Calculul de rezistenta in constructia de masini, vol I, Bucuresti, Editura tehnica, 1960
- [5.] Voinea Radu., Mecanica teoretica, Bucuresti, Editura tehnica, 1968.

J. VLADIĆ

RESEARCH

Influence of Tribological Processes on The Safety Concerning The Slipping of Steel Rope over The Driving Pulley

The system of frictional power transmission through the driving pulley is applied in mechanisms for lifting and moving of load in transport machines, where the load displacement is required to be large. The reliability of such machines is greatly influenced by the safety of power transmission between the steel rope and driving pulley. This feature is especially apostrophed on the machines which perform the passenger transport, such as elevators and ropeways. Safety of power transmission process is defined through the safety factor against slipping on which, among other factors, significant influence has the friction coefficient between the contact surfaces of steel rope and driving pulley. In the paper the influence of the way of contact and the wear of contact surfaces on the equivalent friction coefficient was analyzed.

The verification of calculation models was made through the comparison of results with the experimental results, achieved through the application of specially designed device for equivalent friction coefficient determination. The procedure for determination of allowed wear of driving pulley with V-shaped groove, under different elevator exploitation conditions, was presented. Also, the value of "static" safety factor against slipping as a function of basic elevator parameters was defined, what is of a great importance for elevators design phase.

Keywords: Driving pulley, friction coefficient, groove wear, elevators, ropeways

1. INTRODUCTION

Tribological processes (friction and wear) are of essential importance for safety in exploitation of transport and lifting machines with driving pulley. Of a special importance is defining the safety conditions regarding the devices for transport of passengers (elevators and ropeways). In aim to hinder the rope slipping over the driving pulley, because of the required safe operation and the desired rope life-time, it is necessary to obtain already in design process the defined conditions which ensure the reliability of power transmission using these elements - these conditions are usually comprised in the term "safety factor regarding rope slipping". Its increasing is obtained by increasing the contact pressure according to the chosen pulley groove shape, but the influence of the increased pulley groove wear has to be taken into account, too. In order to confirm the adequacy of the theoretical considerations regarding the frictional power transmission phenomena, the experimental determining of friction coefficient with various rope diameters and types, groove shapes and contact surface hardness has been conducted.

2. SAFETY FACTOR REGARDING ROPE SLIPPING

Basic characteristic of the driving pulley power transmission is load transfer due to friction, between steel wire rope and driving pulley. Most frequently used expression for the safety factor regarding rope slipping differ from each other as a result of different ways of defining them, but they all define the surplus of the driving pulley drawing ability in relation to the required value under operating conditions:

$$\varphi_1 = \frac{S_2 \cdot (e^{\mu \cdot \alpha} - 1)}{S_1 - S_2} \quad (1)$$

$$\varphi_2 = \frac{S_{1max}}{S} = \frac{S_2 \cdot e^{\mu \cdot \alpha}}{S_1} \quad (2)$$

$$\varphi_3 = \left| \frac{S_1 + S_2}{S_1 - S_2} \right| \cdot \operatorname{th} \left(\frac{\alpha}{2} \right) \quad (3)$$

$$\frac{S_1}{S_2} \cdot \varphi_d \leq e^{\mu \cdot \alpha} \quad (4)$$

where: S_p , S_2 - forces in on-going and off-going rope sections,
 μ - reduced friction coefficient,

Dr Jovan Vladoć, v. prof.
 Faculty of Technical Sciences,
 Trg D. Obradovica 6, Novi Sad

α - wrapping angle on the driving pulley,

$\varphi_d = \frac{g+a}{g-a}$ - dynamic factor,

a, g - pulley acceleration and gravitational acceleration, respectively.

For all of these equations minimal required values must be known. The comparison between their limit values, according to their definitions, shows the considerable differences between the corresponding sizes of the safety regions which prevent the rope slipping over the driving pulley. The increase of the driving pulley drawing ability can be obtained by increasing: the tension force in the other rope end (S_2), friction coefficient (μ) or wrap round angle (α). But each of these possibilities represents the complex system of interactive influencing factors. This paper deals with the influence of the equivalent friction coefficient only. Its increasing is obtained by increasing the contact pressure according to the chosen pulley groove shape, but the influence of the increased pulley groove wear has to be taken into account, too. In aim to confirm the adequacy of the theoretical considerations regarding the frictional power transmission phenomena, the experimental determining of friction coefficient with various rope diameters and types, groove shapes and contact surface hardness has been conducted.

According to the deplanation theory [1], the load transfer in driving pulley represents the combination of two limit cases - the states of the elastic slipping of the first and of the second kind.

This model of load transfer phenomena can be used also for explaining the forming of corresponding angles of slipping and relative standstill on a driving pulley, in cases of greater (Fig.1a) and smaller force (Fig.1b) in the coming rope end in comparison with a force in the leaving rope end regardless the ratio of forces in coming and leaving rope ends.

2.1. Pulley drawing ability and equivalent friction coefficient

Driving pulley drawing ability can be defined as a ratio of maximum possible force in the coming rope end and a force in the leaving rope end:

$$C = \frac{S_{1max}}{S_2} = e^{\mu \cdot \alpha} \quad (5)$$

what as the boundary value corresponds to the expression (4).

According to eq. (2), the increase of the driving pulley drawing ability can be obtained by increasing the friction coefficient or wrap round angle or indirectly by increasing the contact pressure between rope and pulley (using special snatching devices, auxiliary ropes, etc.). The influence of the pulley groove shape is here discussed,

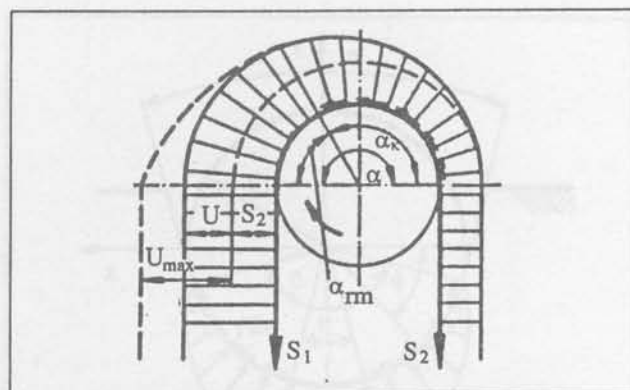


Figure 1. Distribution of forces and characteristic regions on the driving pulley

because of its frequent use in pulleys of vertical lifting systems.

The possibility of power transmission using driving pulley, as a function of groove shape, is usually expressed through the value of equivalent friction coefficient. The contact pressure distribution between the rope and the driving pulley is as usually presumed to be the form of a sinus - function [Thiman 1982]:

$$p = p_m \cdot \sin \varphi \quad (6)$$

with: p_m - maximal pressure value.

This assumption satisfies only for approximate describing of a real distribution. It stands in a relatively good accordance with experimental results for flat contact, rounded groove and rounded groove with narrow undercut. Using of this distribution for rounded groove with wider undercut and for V-shaped grooves leads to considerable disagreement with experimental results because of the neglected influence of rope cross-section deformation. On the basis of the force equilibrium in a radial cross-section of a rounded groove with an undercut (Fig.2.) as a universal groove shape that contains the characteristics of all other groove shapes, the common expression for the equivalent friction coefficient is:

$$\mu = \frac{4 \cdot \mu_0 \cdot \sin \frac{\delta}{2} - \sin \frac{\beta}{2}}{\delta - \beta + \sin \delta - \sin \beta + \mu_0 \cdot (\cos \beta - \cos \delta)} \quad (7)$$

The expressions for equivalent friction coefficient for the groove shapes are:

► V-shaped

$$\mu = \frac{\mu_0}{\sin \frac{\gamma}{2} + \mu_0 \cdot \cos \frac{\gamma}{2}} \quad (8)$$

► rounded

$$\mu = \frac{4 \cdot \mu_0}{\pi + 2 \cdot \mu_0} \quad (9)$$

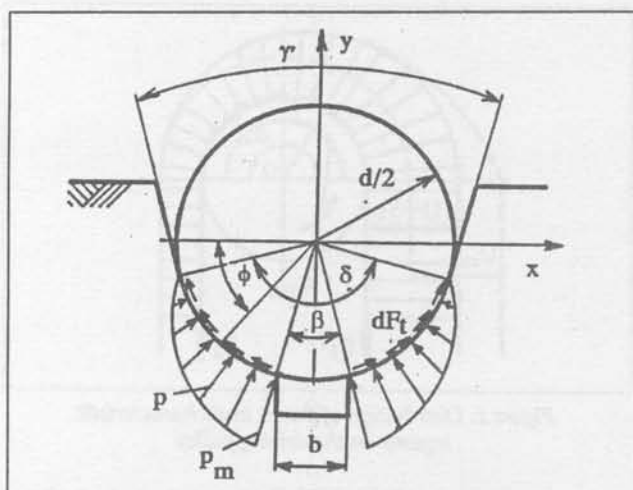


Figure 2. General computation model

► rounded with undercut

$$\mu = \frac{4 \cdot \mu_0 \cdot \sin \frac{\delta}{2} - \sin \frac{\beta}{2}}{\delta - \beta + \sin \delta - \sin \beta + \mu_0 \cdot (\cos \beta - \cos \delta)} \quad (10)$$

The equations are acquired based on the equations (8-10), by omitting the elements with μ_0 .

2.2 Influence of groove wear on the equivalent friction coefficient

It is necessary to analyze the influence of groove sides wear on the pulley drawing ability, i.e. on the value of equivalent friction coefficient. Fig.3 shows two characteristic cases of wearing the contact surfaces of such grooves. On the basis of Fig.3 the characteristic angles can be expressed as:

$$\delta = \begin{cases} \pi - \gamma + 2 \cdot \arccos \left(1 - \frac{2 \cdot k}{d} \cdot \sin \frac{\gamma}{2} \right) & \text{for } k < m \\ \pi & \text{for } k \geq m \end{cases} \quad (11)$$

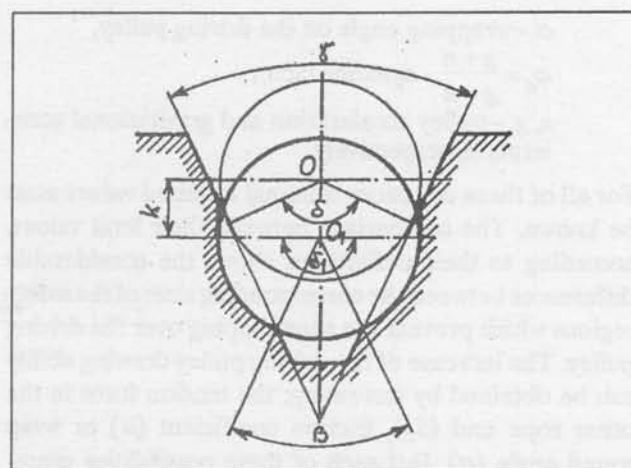


Figure 3. Characteristics of wearing of the V-shaped groove

$$\beta = \begin{cases} \pi - \gamma + 2 \cdot \arccos \left(1 - \frac{2 \cdot k}{d} \cdot \sin \frac{\gamma}{2} \right) \\ 2 \cdot \arcsin \frac{b}{d} \end{cases} \quad \text{for fig. 4b} \quad (12)$$

with:

$$m = \frac{d}{2 \cdot \sin \frac{\gamma}{2}} \cdot \left(1 - \cos \frac{\gamma}{2} \right)$$

Bringing these expressions into the expression (8), for V-shaped groove, enables determining the value of equivalent friction coefficient as a function of vertical displacement of rope cross-section center, which can be used as a measure of groove wearing as shown on diagram in Fig.4 [5].

As a consequence of wearing, the pulley drawing ability decreases during exploitation towards the value for rounded groove. That is the reason for undercutting the V-shaped groove (Fig.4b) with the value of friction coefficient as follows:

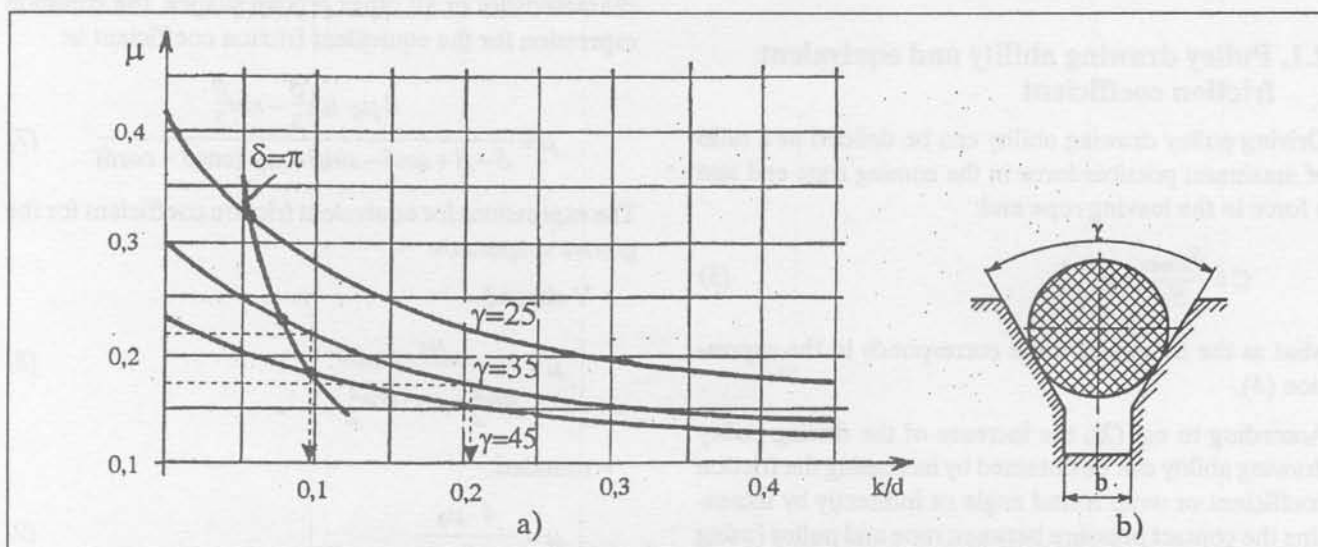


Figure 4. a) Change of the equivalent friction coefficient during wearing of the V-shaped groove and b) V-shaped groove with undercutting

$$\mu = \frac{4 \cdot \mu_0 \cdot \left(1 - \frac{b}{d}\right)}{\pi - \beta - \sin\beta + \mu_0 \cdot (1 + \cos\beta)} \quad (13)$$

with: b - value of undercutting the V-shaped groove.

In aim to proof the adequacy of using the described mathematical model for determining the influence of the contact surfaces shape on the pulley drawing ability and correctness of transfer phenomena assumption, the experiments were performed. Fig.5 shows the experimental device.

In table 1 the average friction coefficient values for the case of new rope and new pulley are shown.

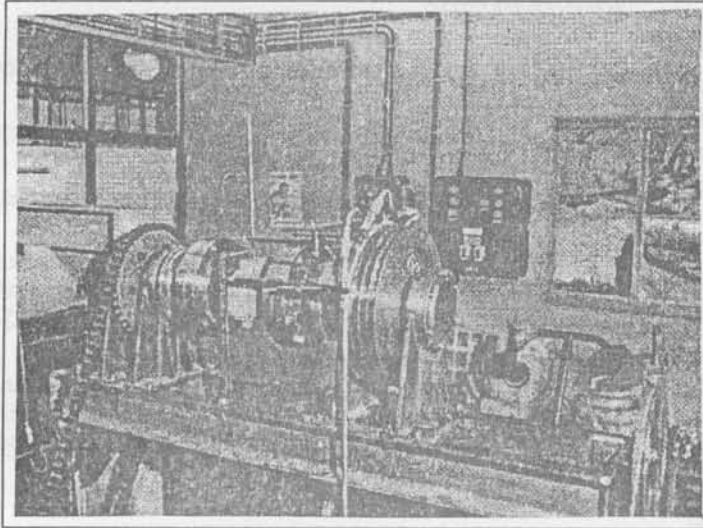


Figure 5. Setup for experimental investigation of the equivalent friction coefficient and wearing groove

Table 1. The average friction coefficient values

Rope	Equivalent coefficient friction	HRC 40				HRC 60			
		flat	V-shaped			flat	V-shaped		
			$\gamma=45^\circ$	$\gamma=35^\circ$	$\gamma=25^\circ$		$\gamma=45^\circ$	$\gamma=35^\circ$	$\gamma=25^\circ$
$\phi 8$, not coated	μ_{SR}	0.238	0.546	0.659	0.735	0.134	0.454	0.646	0.982
$\phi 8$ coated	μ_{SR}	0.278	0.694	0.951	1.022	0.113*	0.720	0.740	**
$\phi 10$, not coated	μ_{SR}	0.237	0.491	0.701	0.804	0.196	0.461	0.665	0.976

* Pulley and rope not sufficiently greased, ** No results obtained, rope tended to get "wedged" in the groove

3. DETERMINATION OF REDUCED FRICTION COEFFICIENT LIMIT VALUES AND SECURITY COEFFICIENTS

Using the expressions (1)-(4) the reduced friction coefficient limit values and safety coefficient against slipping of the rope on the driving pulley can be determined.

According to the expression (2), minimum reduced friction coefficient value, which still provides that the rope does not slip over the pulley is:

$$\mu_{min} = \frac{1}{\alpha_k} \cdot \ln \left[\left(\frac{S_1}{S_2} \right)_{ST} \cdot \varphi_d \right] \quad (14)$$

where: $\alpha_k^{max} \approx 0.92 \cdot \alpha$ - maximum allowed value of elastic slipping on the contact length rope - pulley - force ratio for the on-going and off-going rope section for the case of static load.

On the base of real load values and the shape of rope-pulley contact for the certain case it is possible, under the application of equation (14) and of diagram shown in fig. 4, to determine maximum allowed wear of pulley working surface (for V-shaped groove) and the moment when it is necessary to replace worn out pulley. For instance, for the basic elevator parameters:

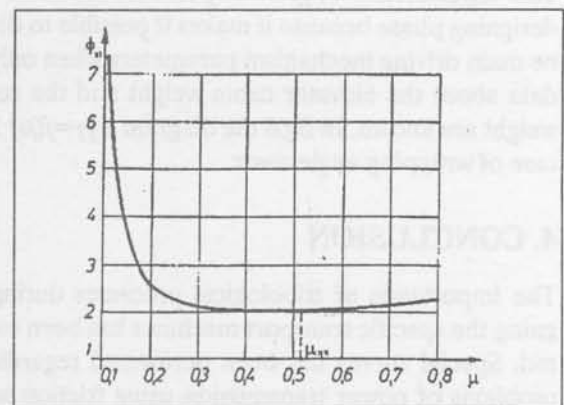


Figure 6. Value for static safety coefficient against slipping

$$\mu_0 = 0.09, \quad \gamma = 35^\circ, \quad \left(\frac{S_1}{S_2} \right)_{SR} = 1.5, \quad \alpha = \pi,$$

$$a = a_{MAX} = 1.4 \cdot \frac{m}{s^2}$$

and rope diameter $\phi 12$ mm, allowed wear is $k = 0.72$ mm with reduced friction coefficient value $\mu_{min} = 0.21$. On the other side, for the same elevator parameters, under the acceleration limitation (for instance through the application of the new flywheel or new control device) on the value of $a = 0.5 \cdot \frac{m}{s^2}$ allowed wear is $k \approx 2.4$ mm with redu-

ced friction coefficient value $\mu_{MIN} = 0.173$. It should be noted that exceeding of limit wear values of pulley working surface does not affect elevators functioning safety, but leads to speedy wear progress of rope and pulley, what in the exploitation leads to the misalignment of elevator cabin floor to the building floors, even with loads which are less than nominal load (especially when the cabin is empty).

Based on of expression (1) it is possible to define minimum value for safety coefficient against slipping for static conditions in the form:

$$\varphi_{st} = \varphi_d \cdot \frac{e^{\mu \cdot \alpha} - 1}{e^{\mu \cdot \alpha_k} - \varphi_d} \quad (15)$$

This expression is of great importance for the elevator designing phase because it makes it possible to determine main driving mechanism parameters when only basic data about the elevator cabin weight and the counterweight are known. In fig.6 the diagram $\varphi_{ST}=f(\mu)$ for the case of wrapping angle $\alpha=\pi$.

4. CONCLUSION

The importance of tribological processes during designing the specific transport machines has been considered. Special survey has been performed regarding the problems of power transmission using friction and the influence of contact surface wearing on the driving pulley drawing ability. The procedure for determining the real

values of equivalent friction coefficient for different pulley groove shapes has been shown.

It is of a great importance to be able to accurately determine the moment when it is going to be necessary to replace the worn out pulley with the new one. It is possible to achieve that through the determination of the allowed wear (k) for given elevator driving mechanism parameters.

Separate problem, only mentioned in introduction, is determining of competent values of safety factor regarding rope slipping as an important parameter for designing machines with driving pulley.

REFERENCES

- [1.] Andreev, A., Friction transmissions, Machinostroenie, Moskva, 1978.
- [2.] Jost, H., Economy impact of Tribology, Proceedings of 20th Meeting of M.F.P.G., 1976.
- [3.] Thieman, H., Aufzuge, Veb Verlagstechnik, Berlin, 1982.
- [4.] Vladic, J., Sovilj, B., Tribological characteristics of friction power transmission in special transport machines, Tribology in industry, No.3, 1994, pp 85-93.
- [5.] Vladic J., Sovilj B., Shostakov R., Tribological characteristics of power transmission in systems with driving pulley, ROTRIB '96, Bucharest, 1996., pp 311-317.

Table 1. The average friction coefficient values		Table 2. The average friction coefficient values	
Material	Friction coefficient	Material	Friction coefficient
Steel	0.150	Steel	0.150
Aluminum	0.120	Aluminum	0.120
Copper	0.180	Copper	0.180
Brass	0.160	Brass	0.160
Cast iron	0.140	Cast iron	0.140
Wood	0.100	Wood	0.100
Concrete	0.080	Concrete	0.080
Plastic	0.060	Plastic	0.060
Glass	0.040	Glass	0.040
Ice	0.020	Ice	0.020